Ore Geology Reviews 121 (2020) 103572

Contents lists available at ScienceDirect

Ore Geology Reviews

journal homepage: www.elsevier.com/locate/oregeorev

Significance of granite-greenstone terranes in the formation of Witwatersrand-type gold mineralisation – A case study of the Neoarchaean Black Reef Formation, South Africa

G.T. Nwaila[a,*], R.J. Durrheim[a], O.O. Jolayemi[a], H.K. Maselela[a], L. Jakaitė[b], M. Burnett[c], S.E. Zhang[a]

[a] School of Geosciences, University of the Witwatersrand, Private Bag 3, Wits, 2050, South Africa
[b] Strike-dip.com, Gargzdai 96001, Lithuania
[c] AMC Consultants, Level 7, Nicholsons House, Nicholsons Walk, Maidenhead, Berkshire SL6 1LD, UK

ARTICLE INFO

Keywords:
Gold
Black Reef
Witwatersrand
Zircon
U-Pb dating
Provenance

ABSTRACT

Geological characterisation and U-Pb geochronology of detrital zircon grains has proven valuable in finding potential source terranes of siliciclastic sediments. Sediment transport and reworking from gold-bearing Archaean/Palaeoproterozoic granite-greenstone rocks are significant in the formation of conglomerate-hosted (Witwatersrand-type) gold deposits. We further support this link with an example from the Neoarchaean Black Reef Formation, in the Carletonville Goldfield, South Africa. In this study, the detrital and hydrothermal pyrite grains are petrographically distinguishable. Association of gold with solely detrital heavy minerals such as pyrite and not with hydrothermal minerals is similar to other Witwatersrand-type examples, which were formed during reducing atmospheric conditions from granite-greenstone protosource rocks. Textural evidence, together with gold occurrence data, support gradual homogenisation of primary sedimentological and mineralogical features due to post-depositional alteration. Uranium-Pb dating of the Black Reef Formation detrital zircon grains yields an age between 3149 and 3061 Ma, indicating that that the provenance of Black Reef Formation sediments could have been derived from a mixture of the hinterland proto granite-greenstone rocks, and from the reworking of Witwatersrand auriferous conglomerates. We further infer a favourable palaeo-drainage for primary sedimentary gold deposition from an isopach model and palaeocurrent data. The fluvial origin of the Black Reef Formation basal conglomerate provides an ideal setting for gold mobilisation from the sediment-source rocks. Notwithstanding the contribution of hydrothermal activity, sedimentary processes are interpreted to have been primary in the initial concentration of gold through reworking of the Witwatersrand auriferous conglomerates. This has important implications for the genesis of the younger Witwatersrand-type gold mineralisation. The fact that the Witwatersrand-type gold deposits, a target for exploration, occur spatially and temporally within the Archaean/Palaeoproterozoic geological record demonstrates that the Witwatersrand Basin is not unique in terms of composition and paragenesis, but is unique in terms of physical size and magnitude of its gold and uranium endowment.

1. Introduction

Palaeoplacer deposits are one of the important sources of gold, contributing ~30% of the global gold production to date (Frimmel, 2018). The genetic relationship between the formation of palaeoplacer gold deposits and composition of protosource rocks is a crucial parameter in understanding the metallogeny of conglomerate-hosted gold deposits. Various post-depositional alteration events (e.g. dykes and metamorphic events) have been recorded within conglomerate-hosted gold deposits (Phillips 1987; Sutton et al., 1990; Gartz and Frimmel, 1999; Phillips and Powell, 2015). A combination of the nature of the hinterland, basin evolution and alteration events, provide a starting point for establishing geological models that will be applicable for mineral exploration. Differentiation between the style of gold mineralisation occurring in reduced and oxidised conglomerate-hosted gold deposits, as well as geochemical, metamorphic and sedimentological characteristics, have been previously applied in order to construct genetic models that may be used for exploration purposes (Davidson and

* Corresponding author.
E-mail address: glen.nwaila@wits.ac.za (G.T. Nwaila).

https://doi.org/10.1016/j.oregeorev.2020.103572
Received 6 March 2020; Received in revised form 28 April 2020; Accepted 30 April 2020
Available online 05 May 2020
0169-1368/ © 2020 Elsevier B.V. All rights reserved.

Cosgrove, 1955; Button and Tyler, 1981; Maynard et al., 1991; Phillips and Law, 2000; Frimmel et al., 2005). To date, none of these models were successful in finding conglomerate-hosted gold deposits that can match the size of the Witwatersrand Basin. Two classes of the conglomerate-hosted gold deposits have been defined, *viz.* conglomerate-hosted gold deposits that formed in a reducing Archaean atmosphere, and those that formed in oxidising conditions (< 2.4 Ga). It is worth noting that there has been a long-standing debate regarding redox conditions of the atmosphere linked to gold mineralisation. The debate started in the 1950s stemming from whether the atmosphere was reducing or oxidising prior to 2.4–2.0 Ga. Proponents of an oxidising atmosphere argued that the atmosphere had sufficient free oxygen by 3.5 Ga and that iron oxide minerals were stable while uranium would have been highly soluble (Palmer et al., 1987, 1989; Ohmoto, 1996). In contrast, the presence of a reducing Archaean atmosphere is supported by the occurrence of abundant detrital pyrite and uraninite in the Archaean auriferous conglomerates and is interpreted to have been characterised by elevated CO_2, CH_4 and H_2S gases with lower O_2 (< 0.1%) compared to present day levels (Button and Tyler, 1981; Krupp et al., 1994; Farquhar et al., 2000; England et al., 2002; Canfield, 2005; Frimmel, 2005). In the past three decades, the reducing atmosphere hypothesis has gained more support and led to the development of commonly applied genetic and exploration models for conglomerate-hosted gold deposits that were formed during the Archaean, even though some of them remain contested.

In the discussion about conglomerate-hosted gold deposits, the controversy has mainly centred on whether the gold deposits of the Mesoarchaean Witwatersrand Basin were formed by (a) hydrothermal or epigenetic processes (Phillips and Myers, 1989; Barnicoat et al., 1997), (b) placer (Minter, 1978), (c) modified placer (Pretorius 1991), and (d) syngenetic processes (Frimmel, 2014, 2018; Frimmel and Hennigh, 2015; Heinrich, 2015; Horscroft et al., 2011). Despite the fact that the modified placer and syngenetic models have been the most widely accepted in recent years; proponents of the main genetic models listed above have all provided additional evidence in support of their hypotheses. It is the authors' contention that the origin of Witwatersrand gold remains one of the most debatable topics in economic geology. Over a century of debate has yielded thousands of published papers, academic dissertations, books, field guides and even novels (e.g. Gold Mine; Smith, 2006).

The Witwatersrand Basin is located in the centre of the Kaapvaal Craton, South Africa (Fig. 1). The Kaapvaal Craton preserves a record of > 1.5 billion years of geological history (Eriksson et al., 2001; Hunter et al., 2006). It comprises granite-greenstone rocks and sedimentary cover sequences including the Barberton Supergroup (Hofmann et al., 2019), the Dominion Group (e.g. Marsh, 2006), the Pongola Supergroup (e.g. Gold, 2006) (a Witwatersrand correlative, e.g. McCarthy, 2006), and the Ventersdorp (e.g. van der Westhuizen et al., 2006) and Transvaal supergroups (Eriksson et al., 2006). The Kaapvaal Craton hosts numerous orogenic gold deposits, mostly located in Archaean greenstone belts, as well as conglomerate-hosted gold deposits occurring in the Dominion Group, Witwatersrand, Ventersdorp and Transvaal supergroups. The gold endowment and characteristics of the auriferous conglomerates present within the Witwatersrand Basin has led to it being regarded as the most important source of conglomerate-hosted gold deposits currently known.

Several examples of the Witwatersrand-type gold mineralisation having similar characteristics exist, including the Black Reef Formation in South Africa and the Huronian Supergroup in Canada (Mossman and Harron, 1983), both of which contain localised occurrences of economically significant gold concentrations. Although there are similarities between the Black Reef Formation meta-conglomerate and Witwatersrand gold deposits, they also display significant, systematic differences, especially in the mineralogy, ore texture and mode of gold occurrence. In this study, we address the contemporaneity of younger Witwatersrand-type gold deposits using the Black Reef Formation as a case example due to its proximity to the Witwatersrand Basin. We present precise U-Pb ages for detrital zircon grains from the basal conglomerate of the Black Reef using laser ablation inductively-coupled-plasma mass spectrometry (LA-ICPMS). The U-Pb ages are used to understand the nature of the protosource and sediment source material. The new age data, together with the results of prior geochronological studies, are used to evaluate relationships between hinterland composition, regional tectonic evolution and the formation of conglomerate-hosted gold deposits from the Archaean to the Paleoproterozoic eras.

2. Geological setting

2.1. Regional geology

The Kaapvaal Craton covers an area of approximately 1,200,000 km^2 and is part of one of the largest and oldest cratons, containing a plethora of mineral deposits including gold, platinum group elements (PGEs), base metals and non-ferrous metals that are hosted in several Archaean basins occurring in distinct cratonic terranes. Prominent suture zones, such as the Thabazimbi-Murchison Lineament and the Colesberg Lineament (Fig. 1), sub-divide these cratonic terranes. The former formed through the collision of the Witwatersrand Block with the Pietersburg Block, whereas the latter arose from the Witwatersrand Block colliding with the Kimberley Block at 2.93 – 2.88 Ga (Schmitz et al., 2004). The granitic basement of the Witwatersrand Block formed and stabilised between 3.4 and 3.1 Ga (Poujol et al., 2003). One of the oldest basement terranes is the Barberton Greenstone Belt, which is well exposed to the east of the Witwatersrand Basin (Dirks et al., 2013; Dziggel et al., 2010; Dziggel and Kisters, 2019). It is the most prominent of the greenstone belts present in the Kaapvaal Craton and far better studied than the Murchison, Pietersburg, Giyani, Amalia and Kraaipan greenstone belts (Brandl et al., 2006; Poujol and Anhaeusser 2001; Poujol et al., 2003). The craton's maximum and minimum ages are constrained by the 3660 ± 4 Ma Ancient Gneiss Complex in the southern part of the Barberton Greenstone Belt and the 3106 ± 3 Ma Nelspruit Batholith that is intrusive into the 3216 ± 2 Ma foreland basin deposits of the Moodies Group (Eglington and Armstrong, 2004, Brandl et al., 2006).

Several granite-greenstone domes form part of the Kaapvaal basement rocks. The 2023 ± 2 Ma (Kamo et al., 1995) Vredefort meteorite impact is thought to have led to the formation of up-doming structures and exposure of deeply buried basement rocks. The impact of this event exposed a variety of high-grade metamorphic ca. 3100 Ga (Hart et al., 1990) gneisses and migmatites and a low-grade metamorphic (ultra) mafic volcanic unit within the Vredefort Dome, as well as in several other domes, most notably the Johannesburg Dome. The Johannesburg Dome occurs to the northeast of the study area (the Carletonville Goldfield) and consists of tonalite-trondhjemite-granodiorite gneisses (TTG gneiss suite) with ages ranging from 3340 ± 3 Ma to 3114 ± 2.3 Ma (Poujol and Anhaeusser, 2001) and minor mafic and ultramafic rocks, interpreted as remnants of Palaeoarchaean upper mantle or oceanic lithosphere (Poujol et al., 2003).

Unconformably above the basement greenstone-granitoids lies the +2000 m-thick clastic *meta*-sediments and volcanic rocks of the Dominion Group, a metamorphosed (greenschist to amphibolite facies) supracrustal sequence that is interpreted as reflecting the first intracontinental basin formation following crustal amalgamation at ca. 3.1 Ga (Jackson, 1992). The Dominion Group's maximum age is constrained by the youngest detrital zircon age 3086 ± 3 Ma (Robb et al., 1992) in sediments derived from the basement granitiods. Its felsic igneous rocks are considered to be one of the sources of the clastic sediments (including detrital zircons) of the Witwatersrand Supergroup and the Black Reef Formation (Robb et al., 1990). The base of the Dominion Group comprises minor zones of economic U-Au mineralisation developed as pyritic quartz-pebble conglomerate beds of the Dominion Reef (Jackson, 1992).

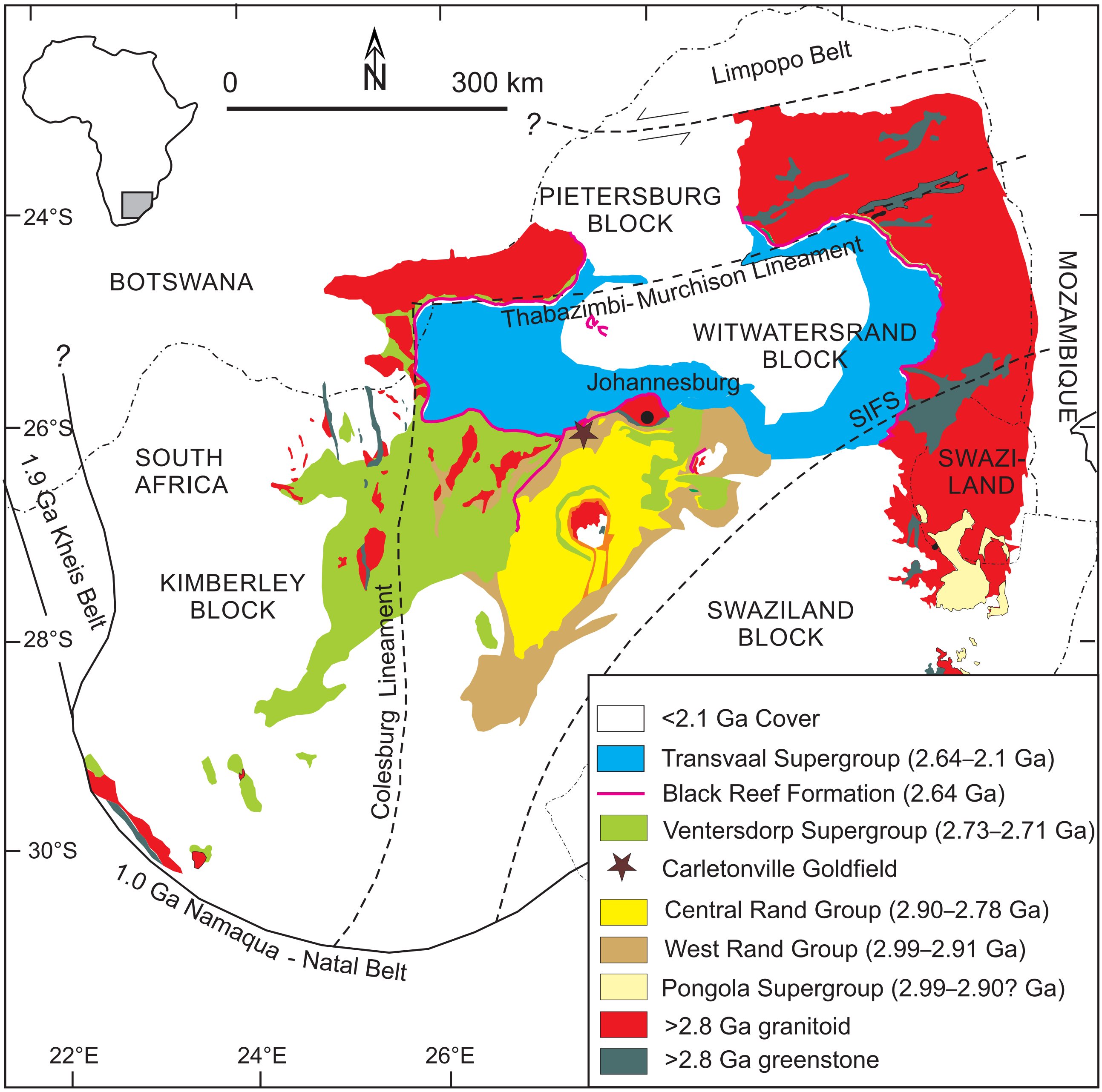

Fig. 1. A simplified geological map of selected basement units of the Kaapvaal Craton and the Witwatersrand Supergroup, showing the extent of the Transvaal Supergroup with special reference to the Neoarchaean Black Reef Formation (modified after Frimmel and Nwaila, 2020).

The gold-rich Witwatersrand Basin lies above the Dominion Group and unconformably above the Kaapvaal Craton's Palaeoarchaean greenstone-granitoid basement. Known as the largest gold province in the world, the Witwatersrand goldfields also constitute one of the world's most significant sources of uranium (Frimmel, 2014, 2018). The Witwatersrand Supergroup extends 350 km in a northeasterly direction and approximately 200 km to the north-west. It is divided into the West Rand Group (2985 ± 14 Ma – 2914 ± 8 Ma; Armstrong et al., 1991) and the Central Rand Group (< 2902 to > 2780 Ma; Kositcin and Krapež, 2004; Gumsley et al., 2018), with over 85% of the known Au-U mineralisation present in the Witwatersrand Basin contained within the Central Rand Group (Fig. 1), which comprises mainly fluvial to fluvio-deltaic sandstones and conglomerates (Frimmel and Minter, 2002). The 2785 ± 1 Ma Ventersdorp Supergroup lies unconformable above the Witwatersrand Supergroup and the Dominion Group (Gumsley et al., 2018). The basal unit of the Ventersdorp Supergroup consists of a gold-rich quartz-pebble conglomerate bed, known as the Ventersdorp Contact Reef (VCR). Generally, the Ventersdorp Supergroup is composed primarily of flood basalts and minor clastics (Tankard et al., 1982). Mining in the Witwatersrand Basin has long reached maturity, with the remaining resources difficult to extract due to declining ore grades (from > 8 g/t to < 4 g/t Au) and safety concerns (Frimmel, 2018; Nwaila et al., 2019).

The Transvaal Supergroup is a 15 km-thick succession of meta-sedimentary rocks that unconformably overlies the Ventersdorp Supergroup (Button, 1986; Walraven and Martini, 1995; Zeh et al., 2015; Gumsley et al., 2017). The Transvaal Supergroup is divided into the Black Reef Formation (ca. 2.64 Ga; Walraven and Martini, 1995), Chuniespoort (2.588 Ga ± 7 Ma; Martin et al., 1998) and Pretoria groups (2.3 – 2.0 Ga; Button, 1981). Two major igneous events confine sediment deposition in the Transvaal Supergroup, that is, the underlying flood basalts of Ventersdorp Supergroup and the overlying

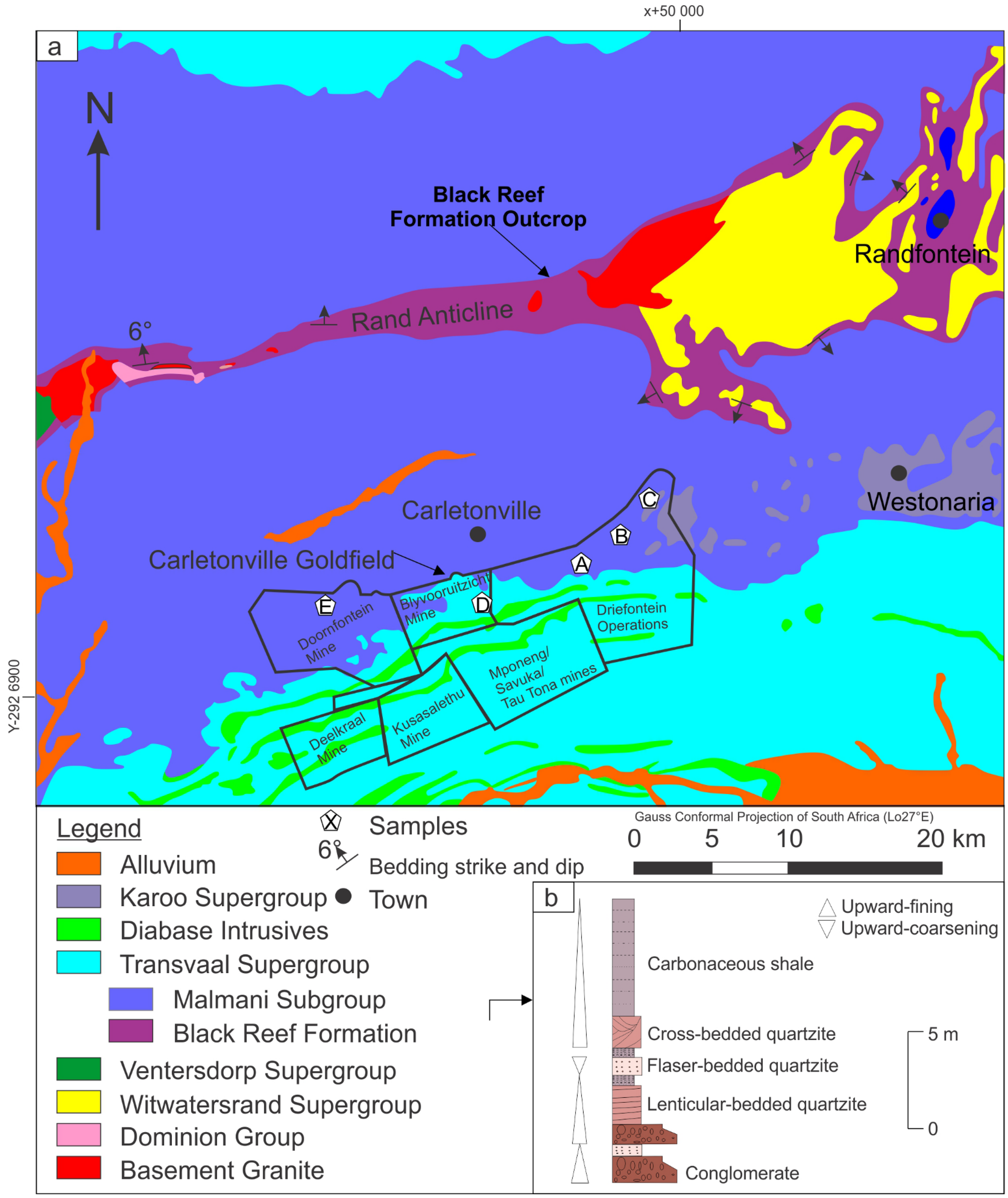

Fig. 2. Geological map (surface distribution) of the pre-Transvaal Supergroup stratigraphic units and outcrops of the Black Reef Quartzite Formation, showing location of the Carletonville Goldfield (modified after Coetzee, 1996). A. Labelled pentagonal shapes indicate the location of the samples; B. A lithostratigraphic column of the Black Reef Formation in the study area.

volcanic rocks of the lower parts of the Rooiberg Group. The Rooiberg Group is followed by (ultra)mafic and felsic rocks of the Bushveld Igneous Complex (2054.8 ± 0.3 Ma – 2055.9 ± 0.3 Ma; Zeh et al., 2015). The development of the Neoarchaean–Palaeoproterozoic Transvaal Supergroup is thought to have been brought about mainly by magmatic events and palaeoclimate change, with tectonics playing a minor role (Gumsley et al., 2017). Exposures of the Transvaal Supergroup occur in the Griqualand West Basin in the southwest of the Kaapvaal Craton, the Kanye Basin to the west of the Transvaal Basin in Botswana, and in the north-northwest, the Transvaal Basin, which is the focal area of this study. Note that each basin of the Transvaal Supergroup has its own stratigraphic subdivision (Eriksson et al., 1995).

2.2. Deposit geology

The earliest records of conglomerate-hosted gold occurrences in the Black Reef Formation are from Stonestreet (1898) and Dorfel (1904). The Black Reef Formation comprises a basal conglomerate followed by interbedded quartz arenites and shales deposited on an uneven palaeosurface. The deposition of the Black Reef Formation and its associated gold content are believed to have been controlled by the uneven footwall topography (Germs, 1982). Conglomerates of the Black Reef Formation are the youngest known auriferous and uraniferous quartz-pebble conglomerate in the Kaapvaal Craton. These conglomerates have been exploited for gold at various localities within the basin, with current exploitation occurring in the Carletonville Goldfields and East Rand (Gauteng province, South Africa). The overlying carbonaceous shale beds are interpreted as having been deposited during a marine transgression (Nwaila and Frimmel, 2019). This led to a higher base level, which resulted in lower sediment flux and eventually in clear water conditions permitting the precipitation of the carbonates that comprise the overlying Malmani Subgroup (Henry et al., 1990;

Clendenin et al., 1991; Eriksson and Reczko, 1995).

Numerous post-depositional alteration events affected the Black Reef Formation. These include regional low-grade greenschist-facies metamorphism, heating during the emplacement of the Bushveld Complex, and the effects of the Vredefort meteorite impact. These events altered the gold-bearing rock units, while the stratigraphic and sedimentological controls on gold grade remained unchanged (Nwaila et al., 2019). Black Reef Formation outcrops, close to the study area, are confined to a topographic ridge (the Rand Anticline), which formed due to the Vredefort meteorite impact (Zhao et al., 2006). Sedimentological characteristics and the origin of Au–U in the Black Reef Formation has been the subject of discussion in numerous publications (Swiegers, 1938, 1939; Frankel, 1940; Liebenberg, 1955; Papenfus, 1964; Frey and Germs, 1986; Van den Berg, 1994; Els et al., 1995; Barton and Hallbauer, 1996; Fuchs et al., 2016; Nwaila et al., 2019). Van den Berg (1994) and Els et al. (1995) conducted sedimentological studies, which found that the palaeocurrent distribution of the basal conglomerate unit is unimodal, while that of the upper quartz arenite is bimodal in specific locations. Frey and Germs (1986) concluded that the gold, present in the Black Reef Formation, is detrital and that the conglomerates were deposited in palaeovalleys. Fuchs et al. (2016) argued and demonstrated that the gold present in the Black Reef Formation was hydrothermally recycled from the Witwatersrand reefs. A recent study by Nwaila et al. (2019) re-emphasized that the primary control on gold grade is sedimentological with the gold introduced primarily as detrital particles. Local remobilisation occurred due to post-depositional alteration events, further mobilising the gold and associated material such as pyrobitumen and hydrothermal pyrite.

Although the Black Reef Formation has been studied since the 1800s, radiometric ages for this formation are limited. Previous U-Pb and Pb-Pb geochronological studies used pyrite mineral separates to characterise the source area and textural controls on gold deposition (Barton and Hallbauer, 1996; Hofmann et al., 2009; Nwaila et al., 2019). Due to an unfavourable economic condition driven by decreases in gold price, exploitation of the Black Reef Formation ceased, with the exception of mining at Modderfontein East (East Rand Goldfield; Gauert et al., 2010; McLoughlin et al., 2014; Fuchs et al., 2016). Modern exploration for economically viable Black Reef Formation re-started in the 1990s (JCI or Johannesburg Consolidated Investment Co. Ltd.) and continued until the 2000s, resulting in localised selective open pit mining in the Carletonville, Randfontein and Krugersdorp areas (Nwaila et al., 2019). Of these, only the Carletonville Goldfield deposit is currently being mined. Exploration is still active in the Carletonville and West Rand goldfields (Gauteng Province, South Africa).

3. Experimental procedures

3.1. Geological mapping and sampling

The samples used for geological characterisation and zircon U–Pb dating were collected from the Black Reef Formation located in the Carletonville Goldfield (latitude 26°24′S and longitude 27°30′E), ca. 70 km west of Johannesburg, South Africa (Fig. 2). The study area covers an aerial extent of 86 km^2. Samples were collected from five representative basal auriferous conglomerates. Fig. 2 shows the location of the sample sites. All samples comprise of large (> 10 mm; apparent long axis in mm) quartz pebbles embedded in a dark-grey matrix. Mineralogically, the samples comprise quartz-chlorite-muscovite-galena-pyrite-chalcopyrite-pyrrhotite-gold-uraninite-zircon. For a quantitative study of the mineralogy of the Black Reef Formation, see Nwaila et al. (2019). The extracted zircons are mainly from the matrix of the samples. Photomicrographs of typical samples and the specific mineralogy and textural association of the Black Reef Formation are presented in section 4.2 of this paper. Detailed underground geological mapping of the Black Reef Formation was also carried out, involving the record of quantitative and qualitative sedimentological and structural data.

3.2. Zircon preparation

All samples were crushed using a jaw crusher to < 50 mm and milled to a coarse powder (< 500 µm) with a disk mill. Zircon grains were separated using a Wilfley table and heavy liquid (sodium heteropoly tungstate). No magnetic separation was performed in order to avoid introducing an artificial bias (Sircombe and Stern 2002; Andersen et al., 2011). Finally, 200–500 zircon grains were selected from each of the five samples, using a binocular microscope. Selection criteria included turbidity, colour, shape and size. The selected zircon grains were then mounted using epoxy resin and ground to expose their cores. Zircon grains were imaged by cathodoluminescence imaging using a JEOL JSM-6490 scanning electron microscope, with Gatan MiniCL, at the University of Johannesburg, South Africa. This made it possible to characterise internal zoning patterns as well as any fractures and pores in the zircon grains. The zircon grains are transparent to translucent, colourless or light brown, and euhedral. They are generally 100–150 µm long with 2:1–3:1 length to width ratios.

3.3. U–Pb detrital zircon U–Pb dating using LA-ICPMS

The U–Th–Pb measurements were carried out in the Earthlab at the University of the Witwatersrand, using an Australian Scientific Instruments (ASI) Resonetics Resolution 193 nm ArF excimer (SE 155) system coupled to a Thermo Scientific Fisher sector-field ICPMS (Element XR). The U-Th-Pb measurements were performed in both low resolution and electrostatic scanning (E-scan) modes. Data were acquired by single spot analysis (30 µm), using a laser repetition rate of 8 Hz and a fluence of 2.5 Jcm^{-2}. Total signal acquisition time was 65 s to allow data processing and preparation for the next analysis, comprising 15 s of pre- and post-ablation (gas blank) and 20 s of ablation measurements. Laser sampling took place in a SE155 dual-volume ablation cell (Laurin Technic, Canberra, Australia) using a mixed He-Ar atmosphere and a small volume of N_2 to enhance signal stability and sensitivity. The following gas flows were applied: He (300–400 ml/min), Ar (800–1200 ml/min) and N_2 (2–4 ml/min), respectively. Zircon standard GJ1 (Jackson et al., 2004) was used for calibration purposes. Temora-2 (Black et al., 2003, 2004) and Plešovice (Sláma et al., 2008) zircon certified reference materials (CRMs) were analysed as unknowns in order to determine the instruments accuracy and precision. The LA-ICPMS system was tuned during line scans using NIST 612 glass for maximum sensitivity for ^{238}U and ^{206}Pb, while maintaining oxide levels (ThO^+/Th) < 0.5% and the Th/U ratio > 0.8. Typically, two analyses of the primary calibration standard were obtained at the beginning and at the end of a sequence. Ten to twenty of the unknowns (CRMs) were followed by the analyses of one primary calibration standard and two to four secondary standards as part of the quality control procedure. Prior to each spot analysis, surface material was removed using two laser pulses. The following masses were measured (six samples per peak): ^{206}Pb, ^{207}Pb, ^{208}Pb, ^{232}Th, ^{235}U, and ^{238}U. Magnet settling time was 0.001 s, and sample times range from 0.0002 s (^{235}U) to 0.003 s (^{207}Pb). All isotopes were measured in pulse counting mode, except for ^{238}U (which was measured in analogue mode).

Data reduction was performed using the Iolite version 3 extension (https://iolite-software.com) to the Igor Pro software (http://www.wavemetrics.com), proceeding in a series of sequential steps, including data import, selection of integrations, baseline subtraction, drift and down-hole fractionation, calibration and error propagation (Paton et al., 2010, 2011). Additionally, the data reduction scheme (DRS) VisualAge (Petrus and Kamber, 2012; http://www.japetrus.net/va) was applied to select integrations more carefully in order to minimise discordance. Graphic presentation and calculation of concordia ages were carried out using ISOPLOT-R software (Vermeesch, 2018). Age distribution histograms were fitted using Gaussian kernel density estimates (Wasserman 2006; Vermeesch, 2012). Empirical cumulative distribution functions (ECDF; Wasserman, 2006) were carried out using

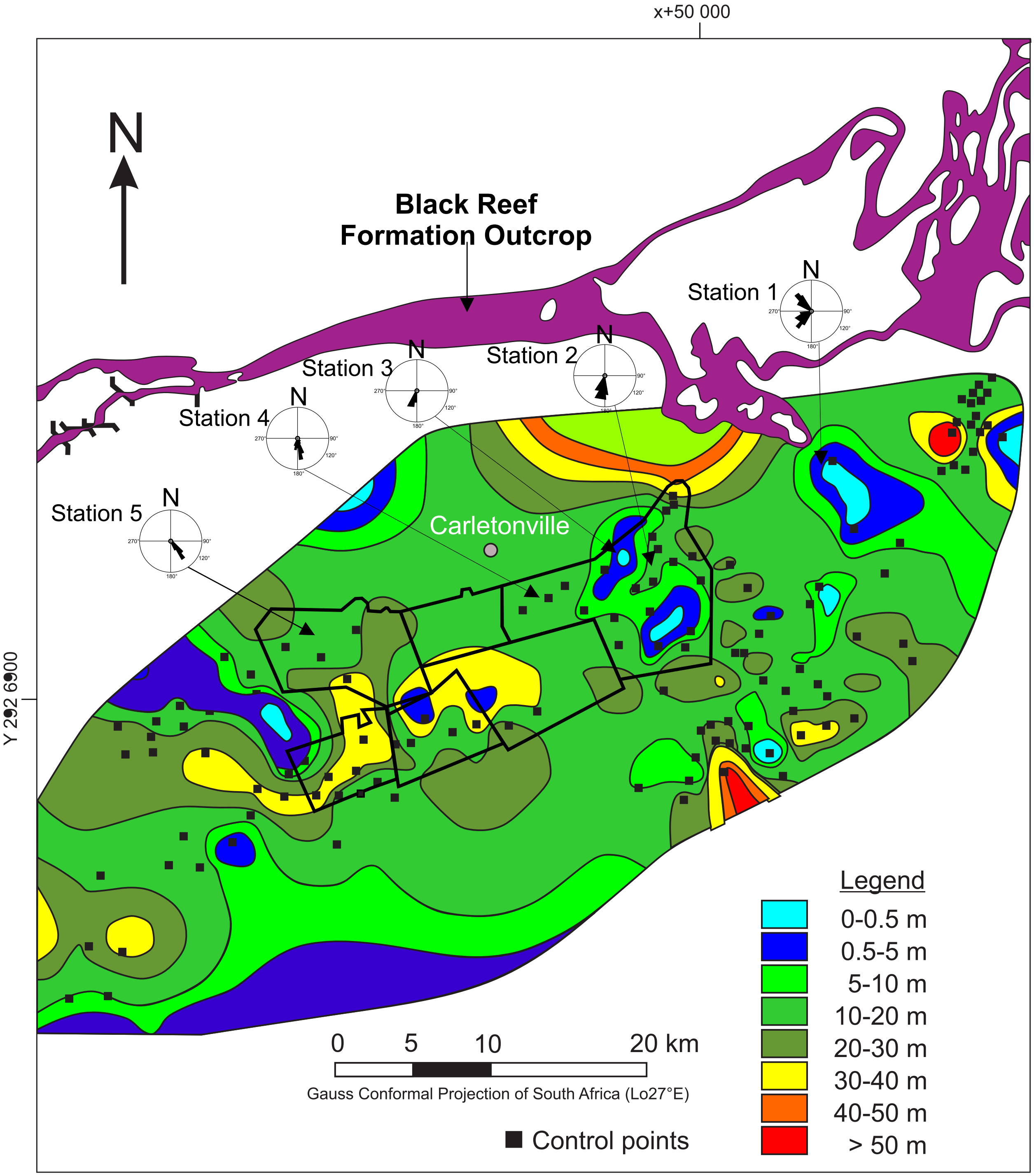

Fig. 3. An isopach and palaeocurrent direction indicators map of the Black Reef Formation in the Carletonville Goldfield. Control points of the isopach map are from a total of 250 borehole intersection archives obtained from Visser (1989); Coetzee (1996) and Sibanye-Stillwater Limited's Oberholzer Geological Centre located in Carletonville.

the 'detzrcr' software package developed by Kristoffersen (2017) and described in Andersen et al. (2017). Uncertainties on individual and mean/regressed ages are 2SE (standard error, absolute).

4. Results and discussion

4.1. Stratigraphic thickness and palaeocurrent direction indicators

The Black Reef Formation, in the study area, displays an upward fining succession with conglomerates forming the base of the formation, which then grades into quartz arenites. Carbonaceous shales overlie the succession occurring above the quartz arenites (Nwaila et al., 2019). The thickness of the Black Reef Formation varies significantly in the study area and appears to be footwall controlled. This evident from variable sediment infill in topographical highs/lows in the paleo-landscape. An isopach map showing thickness variation in the Black Reef Formation was constructed using a combination of surface drill cores, underground drill cores and underground mapping (Fig. 3). This map indicates a lensoidal geometry for the Black Reef Formation in the Carletonville Goldfield, with north–west to south–east trends. The Black

Reef Formation minimum thickness in the study area is < 0.5 m, with a maximum thickness of 70 m recorded (Fig. 3). The maximum thickness observed in this study matches well with measurements recoded by Visser (1989) and Coetzee (1996) in the West Rand Goldfield. The average dip of the Black Reef Formation strata at the Carletonville Goldfield is 7°, thus making it insignificant for tectonic dip corrections. In spite of the sparse number of control points along the margins of the Carletonville Goldfield, due to low number of exploration drill holes, the inward thinning Black Reef Formation, as demonstrated by the goldfield scale isopach map, appears to demonstrate a unitary subsiding, thermal sag basin setting (Bumby et al., 2012). The Black Reef Formation probably represents the last units having strong regional to local topographic influences on sediment accumulation prior to flooding of the Kaapvaal Craton (Sumner and Beukes, 2006).

Palaeocurrent direction measurements were carried out on sedimentary structures, such as trough and cross-bedding, and clast imbrications, in order to determine the direction of sediment transportation. Measurements were taken at five stations (Fig. 3), which correspond to the location of the samples selected for U-Pb age dating except for station 1. Palaeocurrent direction measurements were not taken in the incised channels of the Black Reef Formation, as they are not representative of the local or regional palaeo-drainage patterns. To ensure statistical representability of the measurements, vector mean orientations of the palaeocurrent direction measurements were calculated and plotted as rose diagrams. This analysis demonstrates that sediment sources were located to the northwest and northeast of the study area (Fig. 3). The orientation of palaeocurrent direction indicators shows local sediment source derivation. The evidence gathered from the palaeocurrent direction indicators (Fig. 3) shows the inward direction of sedimentation towards the centre of the Carletonville Goldfield proximal to the Ventersdorp and Witwatersrand supergroups.

4.2. Petrography

The studied conglomerates comprise mainly detrital and authigenic quartz grains, detrital zircon, muscovite, chlorite, monazite, pyrite, gold and uraninite (Fig. 4A and B). Some of the quartz grains contain microfractures. The dominant form of alteration assemblage is chlorite-muscovite-quartz, pyrite, and carbonate. Due to the positive correlation between pyrite and gold (Feather and Koen, 1975), the careful evaluation of the different types of pyrite observed in the basal conglomerate has the potential to provide constraints on the source of the gold in the Black Reef Formation. Three morphological types of pyrite grains were identified from optical microscopy: (I) concentrically laminated pyrite (< 250 μm) with inclusions, (II) irregular to sub-rounded carbonaceous ("sooty") pyrite, and (III) epigenetic pyrite (Fig. 4A and B). We interpret both concentrically laminated and carbonaceous pyrite as allogenic types. Concentrically laminated pyrite grains are rich in gold and other heavy minerals (as micro-inclusions, identified through optical microscopy and/or analysed by SEM-EDS (Nwaila et al. 2019)) such as zircon and are rare when compared to the other pyrite types. The inclusions are arranged in concentric laminae. This pyrite type (Type I) shows mechanical abrasion on the edges and compositional zoning within the grain (Fig. 4B). Carbonaceous pyrite (Type II) grains are large (> 500 μm) and common. They are characterised by small fractures, subhedral rims and surrounded by pyrobitumen. Euhedral epigenetic pyrite grains are scattered within the matrix of the conglomerates (Fig. 4A). Authigenic euhedral pyrite (Type III) is interpreted to have formed in-situ, following deposition (Costa et al., 2020). Since the timing of in-situ pyrite growth cannot be unequivocally determined, both diagenetic and epigenetic pyrite types are referred to as authigenic pyrite. No inclusions of either gold or any other heavy minerals were observed in the authigenic pyrite (Type III) grains. In addition to pyrite, the studied samples contain isolated massive and nodular pyrobitumen. The massive carbon present consists of graphitic carbon (Fig. 4B) and the nodular pyrobitumen. Gold occurs in various forms. It is located in quartz fractures (in the clasts) as specks, and in pyrobitumen and pyrite Type I grain as inclusions. A number of isolated native gold grains (as determined using LA-ICPMS), with irregular morphology, were observed in thin section (Fig. 4A).

4.3. U–Pb zircon ages of Black Reef Formation

The results of LA-ICPMS U–Pb zircon dating for the auriferous conglomerates from the Black Reef Formation are compiled in Table S1. A total of 286 analyses were obtained and 45% of the analysed points (i.e. 128/286) had a concordance level of 95–105%. Only the analyses that meet these 95–105% concordance level criteria were considered for interpretation and discussion. The high degree of discordance in the zircon grain fraction (Table S1) might be due to a long history of irradiation damage and disturbance by later thermal events. 14 out of 128 zircon grain points show $^{207}Pb/^{206}Pb$ ages < 3000 Ma, and the other 114 points give $^{207}Pb/^{206}Pb$ ages ranging from 3009 to 3515 Ma. It should be noted that the $^{207}Pb/^{206}Pb$ age of 3515 Ma is the oldest reported value from the studied samples. The cathodoluminescence images indicated that most of the measured zircon grains contained no inherited cores and that they exhibited good oscillatory zoning, typical for magmatic rocks (e.g. Fig. 5A1 to A5). In addition, there are grains virtually free of any (primary) zoning (Fig. 5B13 and E26), and those showing non-diagnostic zoning (Fig. 5D23). Partially altered grains commonly show porous or re-crystallised domains, which either transect the primary zoning or are concentric to it.

Some grains have undergone complete recrystallisation (Fig. 5E28). Furthermore, a few zircon grains show core-rim relationships (Fig. 5D18 and D20), with rims resulting either from new growth or alteration. Several zircon grains, particularly sample A, show narrow euhedral rims around rounded cores of a few micrometre sizes (Fig. 5A2). For the five analysed samples, the mean $^{207}Pb/^{206}Pb$ age is 3113 ± 20 Ma with a range of 2904–3515 Ma. Fig. 6A to E shows the 'Wetherill' concordia ($^{207}Pb/^{235}U$ versus $^{206}Pb/^{238}U$) diagrams. Individually, sample Tk-10 (Fig. 6A) yielded a concordia age of 3061 ± 6 Ma with a mean square of weighted deviation (MSWD) of 0.22.

Sample Tk-15 (Fig. 6B) yielded a concordia age of 3141 ± 7 Ma (MSWD = 36), while sample Tk-32 (Fig. 6C) produced a concordia age of 3127 ± 4 Ma (MSWD = 0.17). Sample Tk-30 (Fig. 6D) produced three age clusters with a combined concordia age of 3149 ± 4 (MSWD = 4.2). Sample Tk-Sh-38 (Fig. 6E) has a concordia age of 3077 ± 4 Ma (MSWD = 0.13). Quantification of the age relationships, using a likeness parameter (Kristoffersen, 2017) that is not dependent on the number of analyses, revealed that the analysed samples display a strong positive age correlation (r ≥ 0.6). The lowest age correlation (r = 0.6) is between samples TK-32 and TK-10 (Fig. 6F).

4.4. Thorium-to-uranium ratios

Uranium and Th contents of zircon grains from the auriferous conglomerates of the Black Reef Formation are typically in the range of 6–163 and 32–172 ppm, respectively. Age dependency on U or Th content in the zircon grains was not observed in our study. The variation of Th content seems to be higher than that of the U content in individual zircon grains. The Th/U abundance ratio in zircon is sometimes used to distinguish its origin (e.g., Maas et al., 1992). Th/U ratios in igneous zircon grains from various rocks range from 0.2 to 1.0, while zircon grains grown under metamorphic conditions show lower Th/U (< 0.1) (Schiøtte et al., 1988; Kinny and Maas, 2003). It is difficult, however, to distinguish between igneous and metamorphic origins of zircon grains using only the Th/U ratio, as there are exceptional cases of igneous zircon grains with low Th/U (Schiøtte et al., 1988). In this study, Th/U values in all 95–105% concordance level zircon grains (128/128) range from 0.1 to 1.7, and are interpreted as being of igneous origin. Although the Black Reef Formation contains graphitic

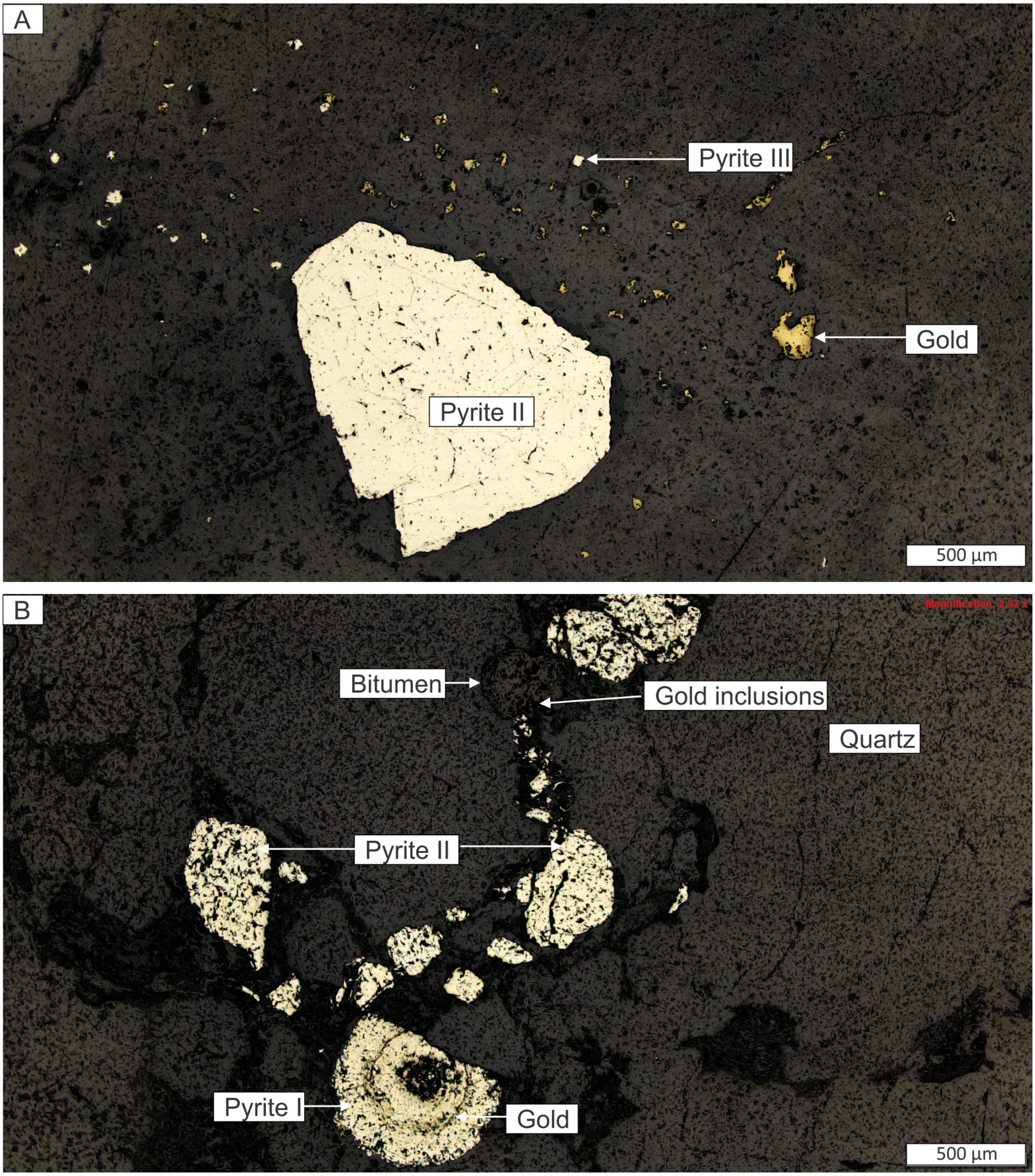

Fig. 4. Reflected-light microscopy photomicrographs of the Black Reef Formation conglomerates showing gold, allogenic- (Type-I and II) and authigenic (Type III) pyrites. Pyrite overgrowing is evident in the Type-II pyrite.

material, evidence that it played a role in creating a significant local reducing environment has not been noticed, thus the Th/U ratios in the zircon grains might not have been heterogeneously disturbed during the later Bushveld Complex magmatic event.

4.5. Degree of discordance (Disc. %)

The degree of discordance for a zircon grain indicates the chronological difference between the two ages determined by Pb–Pb and U–Pb methods, and is defined as {1-(^{206}Pb/^{238}U age)/(^{207}Pb/^{206}Pb age)} × 100 (%) (e.g., Biao et al., 1996). If the samples were influenced by the metamict effect, the discordance of individual zircon grains would be closely related to their U/Th contents and/or formation ages. Zircon grains with higher Th/U dispersions, ranging from 0.1 to 2.5 (158 of 286) are almost all discordant. Zircon grains that have 95–105% concordance levels have Th/U ratios ranging from 0.1 to 1.7. In addition, a minor age dependence of the concordance can be observed; only 22% of the concordant grains (28 of 128 grains) are younger zircon grains ($\leq$3050 Ma), whereas 78% (100 of 128) are older zircon grains ($>$ 3050 Ma). There is no strong correlation between the age and the discordance. Therefore, the U–Pb disturbances observed in these zircon grains are not caused by the metamict effect.

4.6. Precambrian protosource and sediment source rocks

The protosource rocks of the Black Reef Formation can be mostly explained by the contribution of multiple source rocks that span the

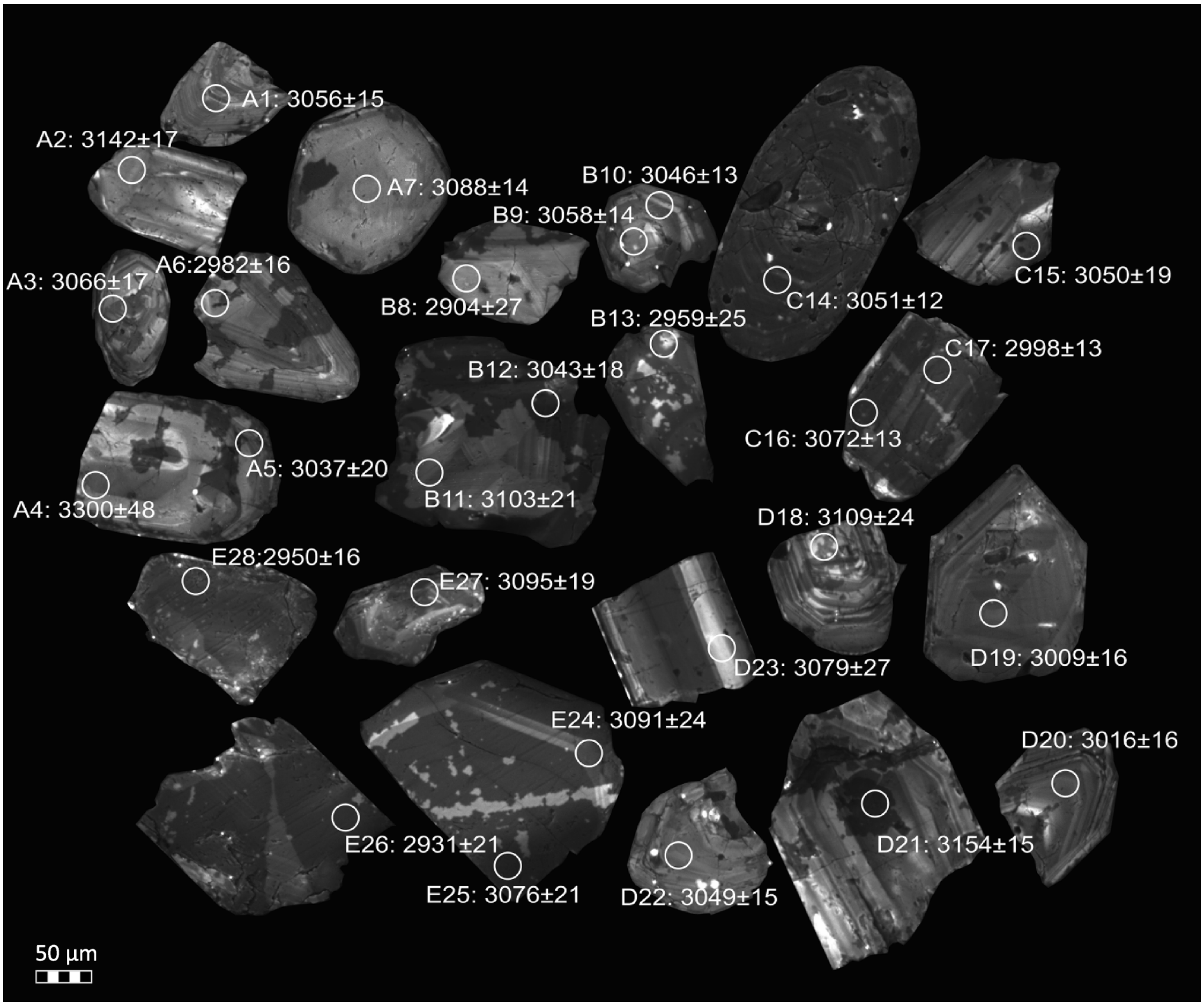

Fig. 5. Cathodoluminescence images of zircon grains from the Black Reef Formation basal auriferous conglomerate. The given spot numbers' ages' are $^{206}Pb/^{207}Pb$ ages in million years. The given spot numbers refer to Table S1.

Palaeoarchaean to Mesoarchaean eras, including the basement granitoid-greenstone rocks. These protosource rocks could include material derived from the Johannesburg Dome, Murchison Greenstone Belt and the Amalia-Kraaipan Greenstone Belt (Brandl et al., 2006). This observation is supported by the Th/U ratio, morphology and size of the studied zircon grains when compared to pre-Black Reef Formation rocks (Kositcin and Krapež, 2004; Koglin et al., 2014). However, the sediment sources are likely to be from the Witwatersrand Basin, due to similarities in the number of zircon modes and overlapping zircon ages between the Black Reef Formation and those recorded from the Central and West Rand groups of the Witwatersrand Basin (Koglin et al., 2010a) – or all those zircon populations came from a common source beyond the Witwatersrand Basin. Zircon grains with ages of < 3000 Ma (Fig. 7) are interpreted as representing sediments recycled from the Witwatersrand Supergroup or Mesoarchaean granites in the hinterland (Kositcin and Krapež, 2004; Gumsley et al., 2018). The lack of < 2785 ± 1 Ma (age of the Ventersdorp Supergroup) (Figs. 7 and 8) zircon grains in this study is not surprising as the Ventersdorp Supergroup consist primarily of continental flood basalts that are barren of zircon. Alternatively, the lack of < 2785 ± 1 Ma zircon grains could be due to the presence of the topographic high, present in the Transvaal Basin at the time, that prevented material being sourced from the north.

Visual comparison of empirical cumulative probability density functions (ECDF) with associated confidence bands give a good indication on the similarity/dissimilarity of the samples and if apparent dissimilarity is real or just an artefact of sampling bias (Fig. 8). From the ECDF plot (Fig. 8), we are certain that the sampled Black Reef detrital zircon grains are representative and provide a good estimate of the source rock zircon age population. The size of detrital zircon grains offers potentially powerful constraints on sediment transport distance and the reconstruction of palaeofluvial systems (Viljoen, 1963; Wernicke, 2011), and may be used to discriminate sedimentary transport from crustal deformation (Renik et al., 2008). Binocular microscope size analysis of the zircon grains (> 300 µm) revealed that they are larger than zircon grains found in rock units of the Dominion felsic volcanic rocks (< 300 µm (Frimmel et al., 2009)). A study by Frimmel et al. (2009) described the presence of granites and hornblende metagabbro, with an estimated age of 3062 ± 5 Ma, in the hinterland of the study area. We infer that some of our zircon grains, with similar ages to those obtained by Frimmel et al. (2009), are likely to have been sourced from these basement granitic rocks.

Witwatersrand rocks, which we interpret as having provided the majority of the sediment load for the Black Reef deposit, were subjected to various cycles of erosion and deformation (Kerr et al., 2017). Some of the erosion produced identifiable features such as erosional channels that would have been very capable of localised gold transport and concentration from proximal sources (Nwaila et al., 2020). Such environments, acting in parallel with geomorphological processes (e.g. seasonal and fluvial-incision; Dunn et al., 2019) permit mechanical recycling of heavy mineral suites, including gold and pyrite. Lead isotope analysis (Barton and Hallbauer, 1996) of the Black Reef Formation detrital pyrite grains revealed that their age and source overlaps with

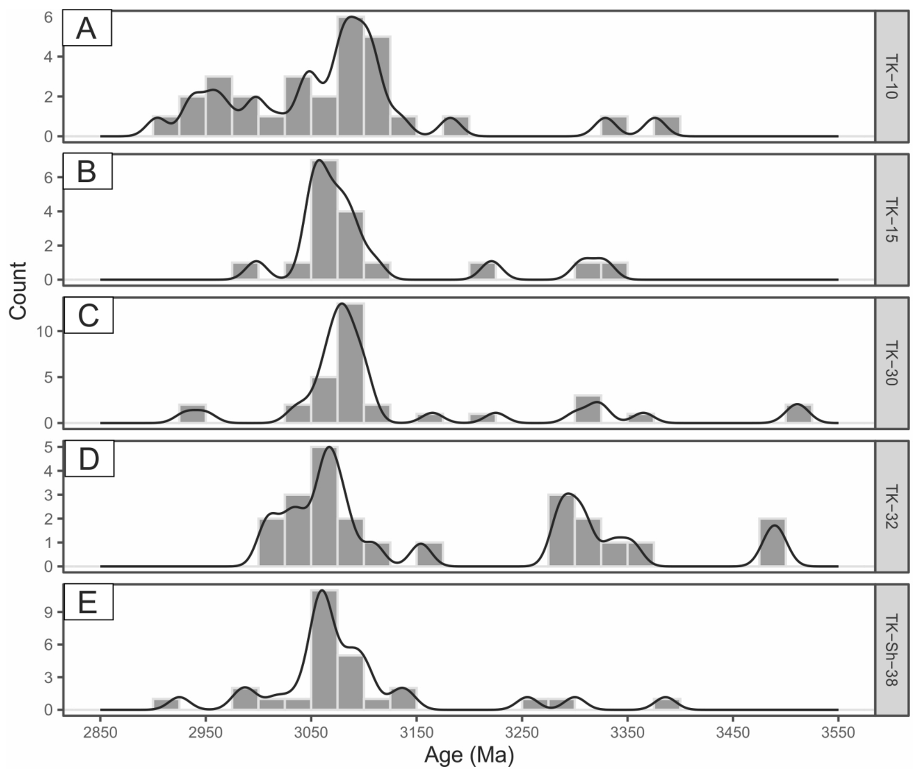

Fig. 6. Results for U–Pb analyses of detrital zircon grains from auriferous basal conglomerates of the Black Reef Formation (A to E). Concordia ages are presented only for the main age fractions (concordance level 95–105%). Error ellipses are plotted as 2σ. Likeliness of the $^{206}Pb/^{207}Pb$ age spectra showing correlation between the studied samples (Fig. 7F) (F).

the detrital zircon ages obtained in this study. A detailed multiple S and Fe isotope analysis (e.g., Hofmann et al., 2009) of allogenic pyrite grains of the Black Reef Formation revealed a mixture of magmatic and sedimentary sources. Nwaila et al. (2019) analysed both allogenic and authigenic pyrite grains for their Re-Os isotopic composition, which revealed a local derivation from the hinterland, overlapping with results from Kirk et al. (2002) and thus supporting the hypothesis of mechanical reworking of Witwatersrand sediments. With regard to uranium mineralisation within the Black Reef Formation, the 3174 ± 9 Ma greisenised granites around Hartebeestfontein (Robb and Meyer, 1995) have been proposed as the main sources of detrital uraninite found in the Witwatersrand Supergroup. The proximity of the Black Reef Formation to the Witwatersrand strata enables derivation of uranium and gold mineralisation as the product of recycling (be it chemical or mechanical derivation) from the hinterland granites into the auriferous conglomerate of the Black Reef Formation. If this is valid, some of the clast assemblage of the Black Reef auriferous conglomerate could also be the product of felsic volcanic rocks from these hinterland granites.

4.7. Significance of gold mineralisation in auriferous conglomerates of the Black Reef

The intimate and necessary link between Archaean protosource rocks, evolution of atmospheric oxygen, development of the juvenile crust, background levels of gold concentrations in the Earth's crust and auriferous conglomerate, provides a platform to assess sediment-hosted gold deposits in time (Fig. 9A to C). The genesis of Witwatersrand-type gold deposits requires several factors to work together or in sequence to facilitate the mobilisation, transport and precipitation of gold (Fig. 9A). The spatial distribution and size of these gold deposits (Fig. 10) suggests that the underlying formational processes of these deposits are not related to a specific time period and they share many similarities aside from the host rocks. The Black Reef, which is considered to be the youngest example of a Witwatersrand-type gold deposit, is one of many occurrences of this style of mineralisation (Fig. 10). The similarities include (a) the composition of the hinterland, (b) mineralogical composition and dependence of paragenesis on atmospheric O_2, and (c) gold concentrating mechanism. Additional detailed characteristics and features of Witwatersrand-type gold deposits including fluid chemistry, alteration assemblages, geochemistry, basin analysis and structure are described and summarised in Barnicoat et al. (1997); Frimmel et al. (2005); Frimmel (2014; 2018); Frimmel and Nwaila (2020); Kirk et al. (2002); Large et al. (2013); Law and Phillips (2006); Phillips and Law (1994, 2000) and references therein. Witwatersrand-type gold deposits are further characterised by the presence of carbonaceous matter in the conglomerate horizons, as seams and nodules (see England et al., 2002; Frimmel et al., 2005; Mossman et al., 2008; Fuchs et al., 2016, 2017). We will only discuss genetic similarities and apparent variations in mineralisation style of the Black Reef Formation deposit.

4.7.1. Composition of the hinterland

Most known occurrences of Witwatersrand-type gold deposits are associated with Archaean/Palaeoproterozoic granite-greenstone terranes (Fig. 9A; Robb et al., 1990; Law and Phillips, 2006; Frimmel et al., 2005). Some of the basement rocks are important sources of orogenic gold, which is hosted in the basement greenstones of the Archaean cratonic nuclei (> 3 Ga) and Palaeoproterozoic mobile belts. Notable examples are the gold deposits of the Barberton Greenstone Belt, South Africa and the Ashanti Belt in Ghana. A number of small gold occurrences have been reported in the Sutherland, Pietersburg and Murchison greenstone belts, South Africa (de Wit et al., 1993). In the context of the Black Reef Formation, our detrital zircon ages have shown that the protosource rocks are derived from a suite of Archaean granite-greenstone basement rocks.

A comparable composition of the protosource rocks has been described in the 2.65 Ga Moeda Formation, Brazil. The Moeda Formation is a meta-sedimentary clastic sequence of Witwatersrand-type conglomerate and quartz arenites occurring at the base of the Neoarchaean to Palaeoproterozoic Minas Supergroup, Quadrilátero Ferrífero of Minas Gerais (Koglin et al., 2014). Gold in the Moeda Formation is mined from basal pyrite-bearing meta-conglomerates (Garayp et al.,

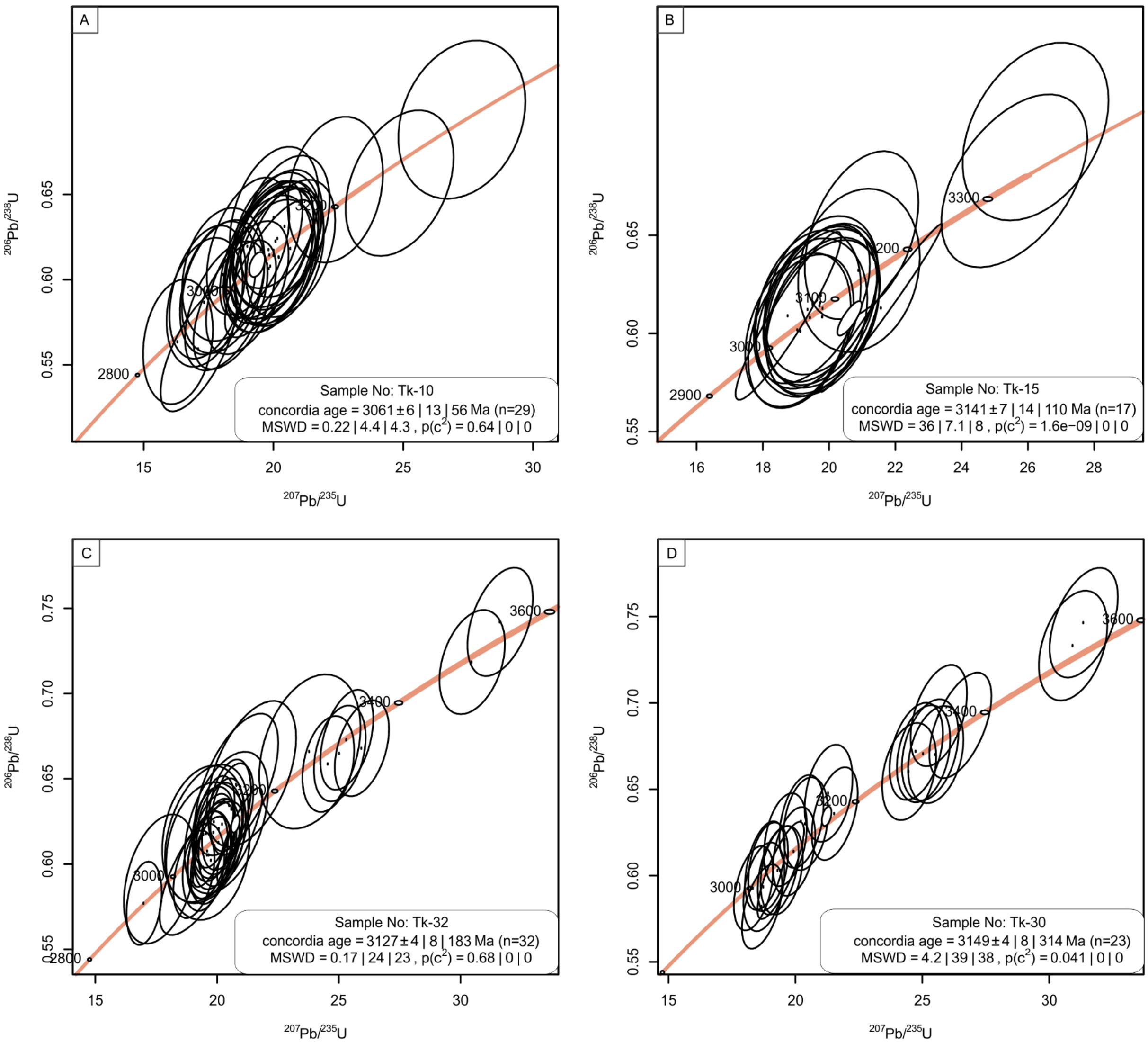

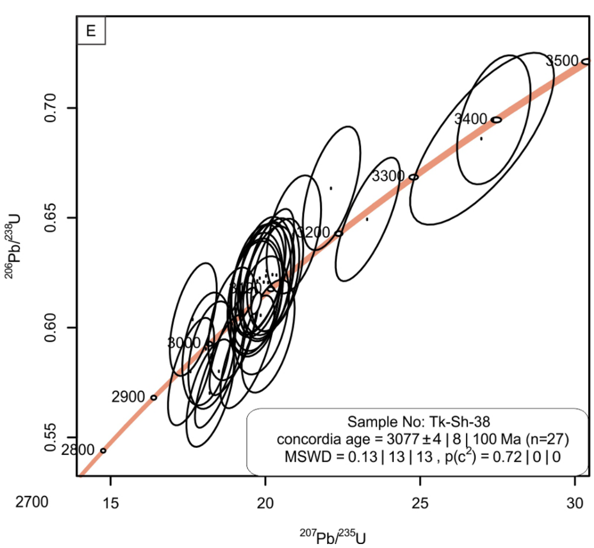

F

207Pb/206Pb age (Ma)	TK-10	TK-15	TK-30	TK-32	TK-Sh-38	All 95-105 % conc.
TK-10	1.0	0.7	0.8	0.6	0.8	0.8
TK-15	0.7	1.0	0.8	0.7	0.9	0.9
TK-30	0.8	0.8	1.0	0.7	0.8	0.9
TK-32	0.6	0.7	0.7	1.0	0.7	0.8
TK-Sh-38	0.8	0.9	0.8	0.7	1.0	0.9
All 95-105% conc.	0.8	0.9	0.9	0.8	0.9	1.0

Fig. 7. Combined histogram and kernel density estimate plots of $^{206}Pb/^{207}Pb$ age spectra of zircon grains from all studied samples of auriferous conglomerates of the Black Reef Formation with a concordance level of 95–105%. Vertical bars indicate the main age populations. It should be noted that the panels use different y-axis scaling.

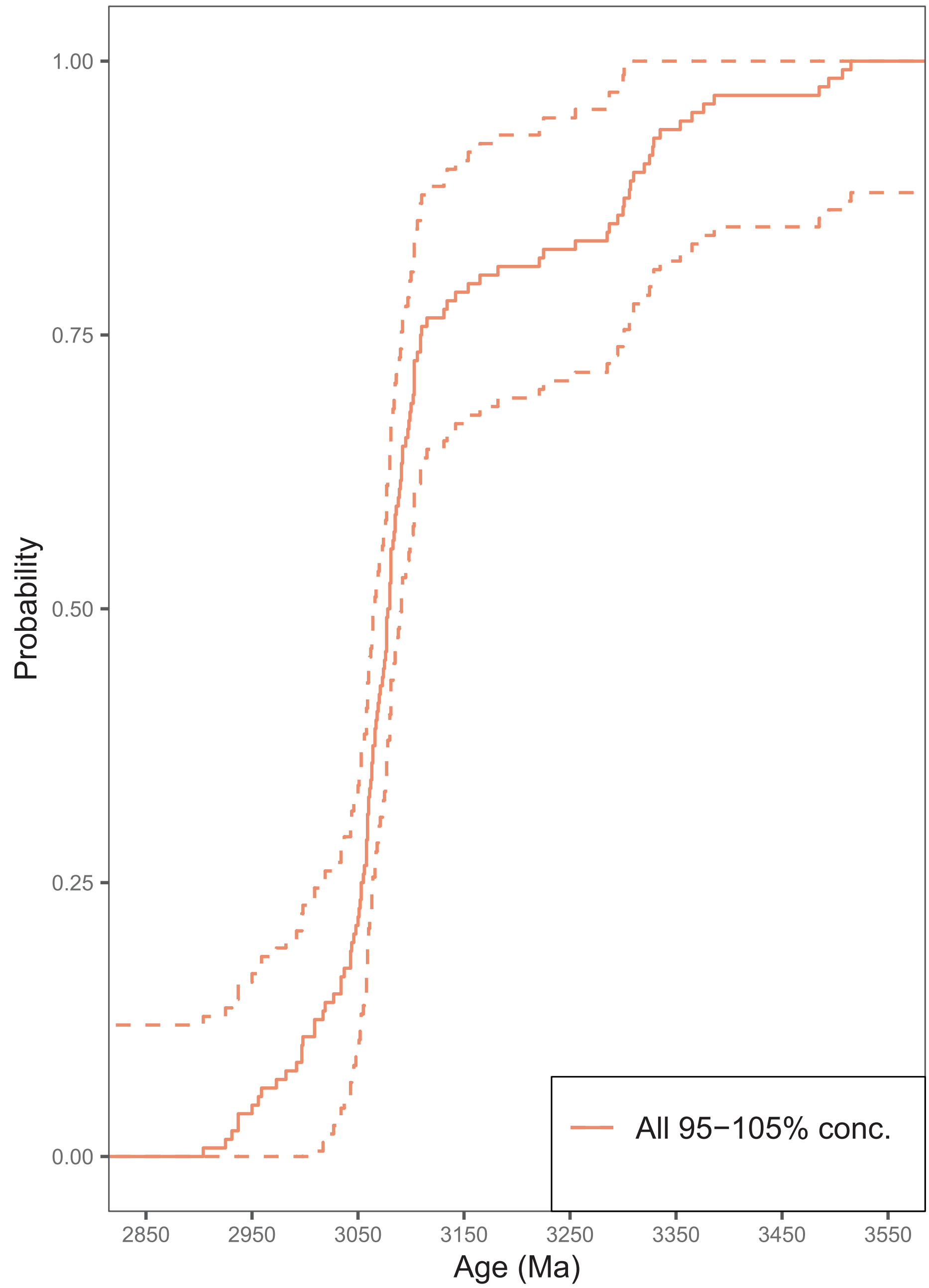

Fig. 8. Plot of the empirical cumulative distribution functions of $^{207}Pb/^{206}Pb$ age spectra (solid line) with associated 95% confidence (dotted lines) bands (Dvoretzky et al., 1956) of the Black Reef Formation.

1991). These conglomerate layers, locally auriferous, occur either as channels on, or in tectonic contact with Archaean rocks of the Nova Lima Group, which forms the upper part of the Rio das Velhas Supergroup (Endo and Machado, 2002). The contact between the latter is marked by an angular and erosional unconformity, a common feature in Witwatersrand-type gold deposits, including the Black Reef Formation (Machado et al., 1996). In contrast to most of the known Witwatersrand-type hinterlands, the detrital zircon populations of the Moeda Formation sediments provide little evidence for juvenile crustal formation in the hinterland, at 2.65–2.61 Ga (Koglin et al., 2014). In the Bahia Province, north-eastern Brazil, the Jacobina Palaeoproterozoic gold-bearing conglomerates are possibly one of the youngest, economically significant, Witwatersrand-type gold deposits; with sedimentation estimated to have occurred between 2086 and 1883 Ma (Milesi et al., 2002), although the Jacobina conglomerates also demonstrates evidence consistent with hydrothermal mineralisation (Milesi et al., 2002). Analogous to the Black Reef Formation, the hinterland comprises granite-greenstone rocks (Pretorius, 1981). The youngest example in Brazil is Roraima, with an estimated U-Pb zircon age of 1901 ± 1 Ma (Milesi et al., 2002), which lies above a basement with high concentrations of gold when compared to both the average Archaean and Bulk Crust standards (Pitcairn, 2011).

In West Africa, Witwatersrand-type gold mineralisation occurs in the 2107 Ma (Perrouty et al., 2012) Tarkwa gold deposit in Ghana, which exploits the Bankets Series (also referred to as Banket Formation) of the Tarkwaian Group, overlying the Birimian Supergroup. The majority of Ghana is underlain by metamorphosed Palaeoproterozoic (2300–1900 Ma) rocks of the volcano-sedimentary Birimian Supergroup and the overlying clastic sedimentary Tarkwaian Group (Oberthür et al., 1998; Griffis et al., 2002) that make up the Man Shield (also known as the Leo Shield) of the West African Craton (Griffis et al., 2002). The Banket Series comprises well-sorted conglomerates and

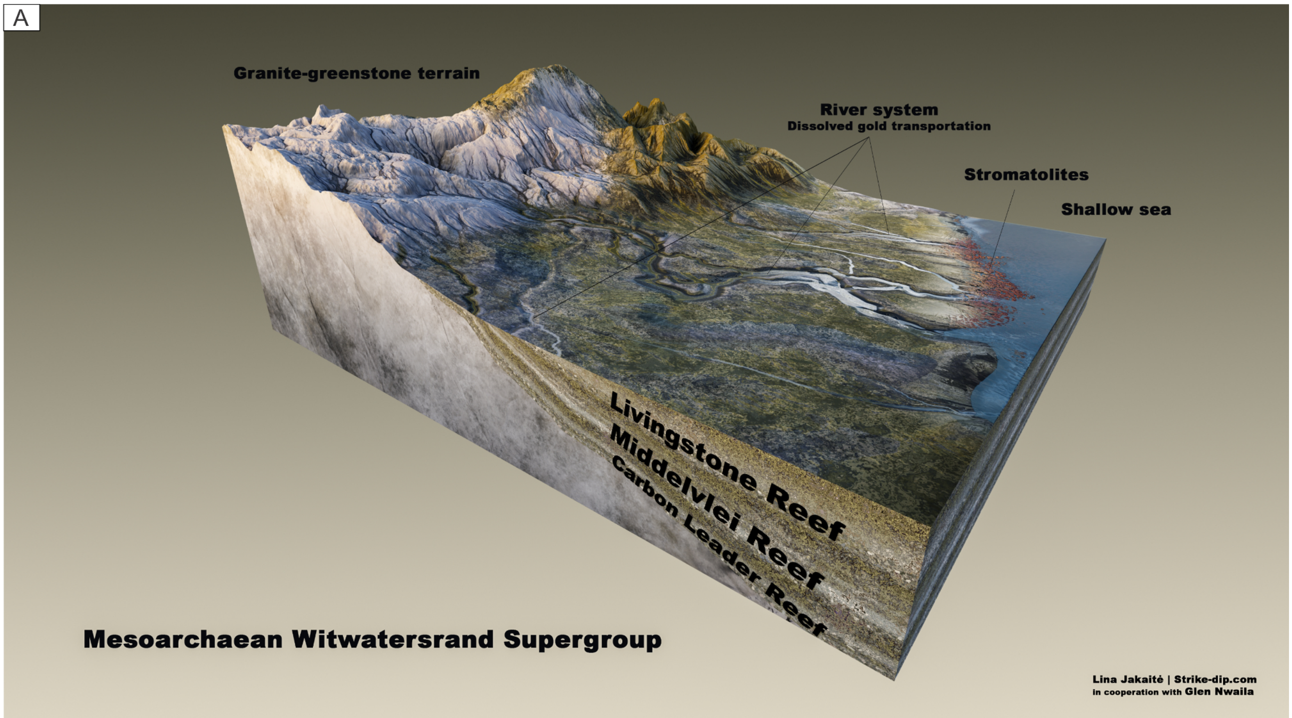

Fig. 9. A. Schematic palinspastic illustration of Archaean granite-greenstone terrane showing sequential processes for the formation of the Mesoarchaean Witwatersrand-type such as the various reefs found in the Central Rand Group. The envisioned Archaean conditions include (i) intense volcanic activity and acidic rains, (ii) lower than present-day levels of atmospheric oxygen (reducing atmosphere before ~2.4 Ga), (iii) transportation of dissolved gold by Archaean rivers from chemically weathered granite-greenstone rocks and quartz veins into shallow sea and oxygenated oceans (Frimmel, 2014; Heinrich, 2015), (iv) gold precipitation and accumulation near shallow lakes facilitated by the presence of early life forms (i.e. stromatolites), (v) reworking of precipitated gold by fluvio-deltaic processes and subsequent distribution into arenitic (quartz arenite) and ruditic (conglomerate) units (Frimmel, 2014, 2018). B. Depiction of the Neoarchaean environments showing the formation of the Ventersdorp Contact Reef (written as "Ventersdorp Reef") and preservation of the Witwatersrand strata by continental flood basalts, an analogy of modern-day Hawaiian, Icelandic volcanism. C. Illustration of the formation of the Neoarchaean Black Reef gold deposit which was brought by further reworking of auriferous conglomerate units of the Witwatersrand Supergroup, Ventersdorp Supergroup and hinterland granites. Note that additional processes such as post-depositional remobilisation of gold have been acknowledged in the text, but have not been included in this palinspastic restoration for simplification.

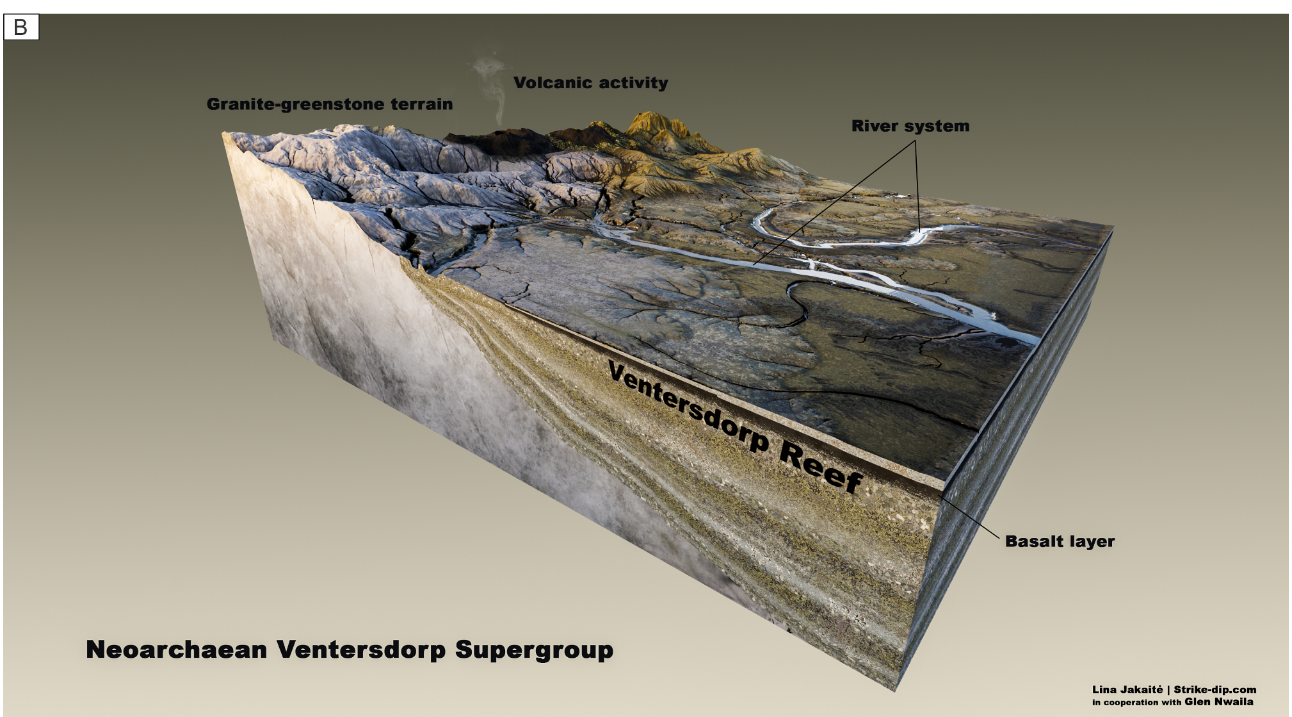

Fig. 9. (*continued*)

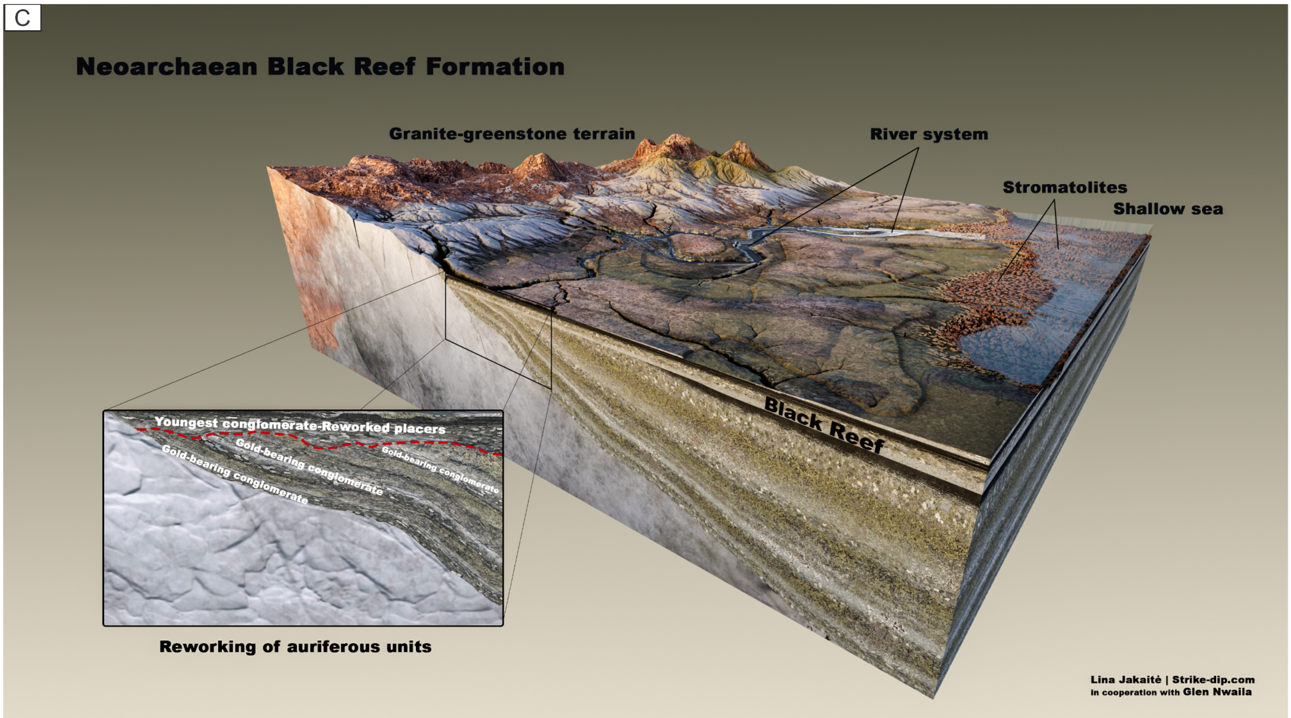

Fig. 9. (*continued*)

quartz arenites, with clasts generally considered to be derived from the Birimian Supergroup, and containing significant gold mineralisation, hosting the Tarkwa orebody (Oberthür et al., 1995). The Tarkwa ore bodies form a significant portion of the stratigraphy of the Ashanti Belt in southwest Ghana (Smith et al., 2016). The Tarkwaian Group in the Ashanti Belt formed in a long, narrow basin, with the western fault-bounded contact forming a half-graben. The contact between the Birimian Supergroup and the Tarkwaian Group is commonly marked by

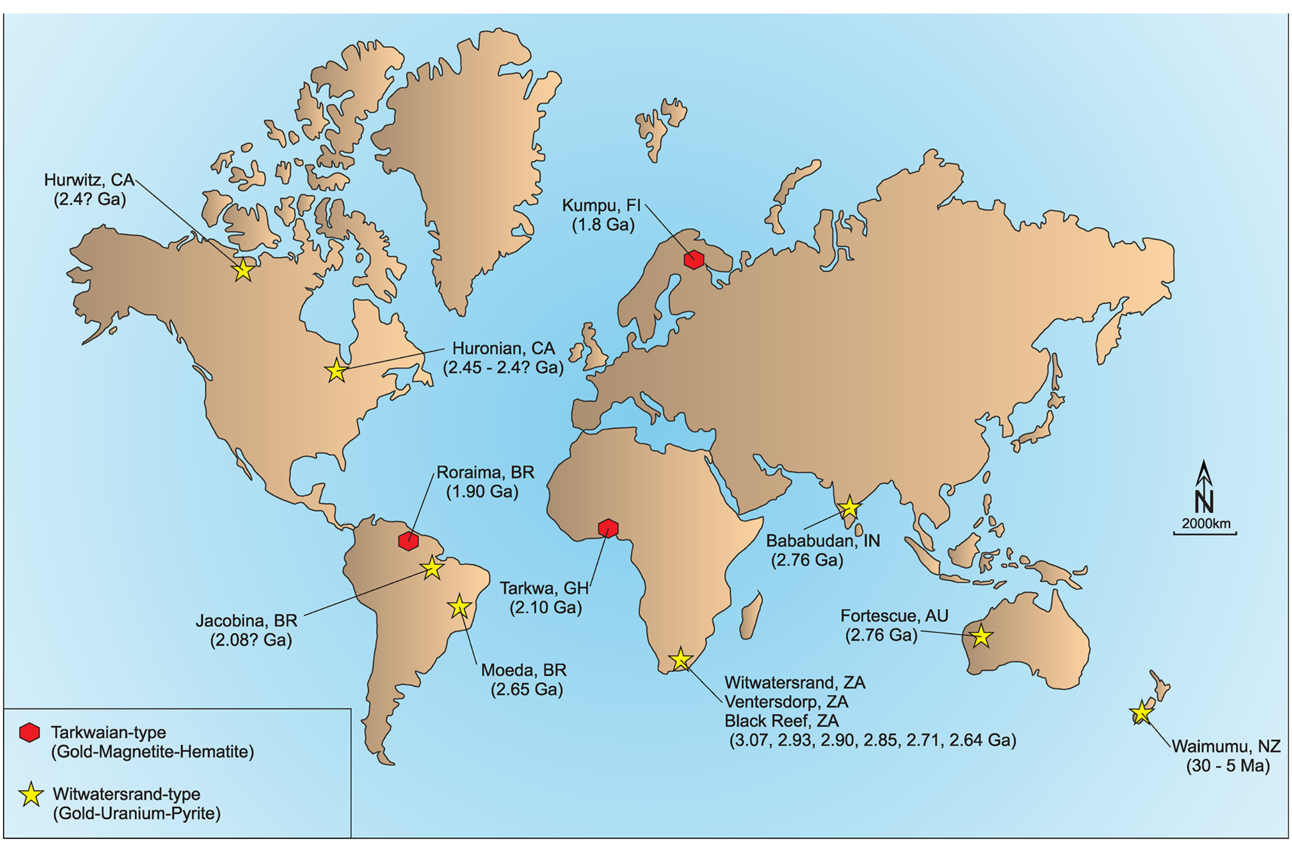

Fig. 10. Geographical distribution of the Witwatersrand-type gold deposits. ZA = South Africa; BR = Brazil; NZ = New Zealand; AU = Australia; IN = India; CA = Canada; FI = Finland; GH = Ghana.

zones of intense shearing and is host to a number of significant shear-hosted gold deposits including Prestea, Bogoso and Obuasi (Yao and Robb, 2000). Similar to the Black Reef Formation, the Tarkwaian Group has been metamorphosed to lower greenschist facies (Griffis et al., 2002). In all the Witwatersrand-type gold deposits/occurrences found globally, the background concentration of gold is higher than the average crust (Nwaila et al., 2017; Pitcairn, 2011; Frimmel, 2018).

4.7.2. Mineralogical composition and dependence of paragenesis on atmospheric O_2

In most of the Witwatersrand-type gold deposits, the primary mineralogical assemblages and textures have been altered by post-depositional tectonothermal events. The starting material, in which the replacement textural features are developed, is highly diverse and includes individual minerals and rock units. Primary minerals are highly variable, the most common being gold, uraninite, pyrite, zircon, quartz, Fe oxides and feldspars. Pyrite is the most noticeable, occurring typically in the matrix of the conglomerate, as layers on foresets within the conglomerate, and in the quartzitic rock of the footwall and hangingwall sequences (Hallbauer et al., 1983). The primary assemblages have been altered to produce metamorphic minerals, typically pyrophyllite–chloritoid–muscovite–pyrite-chlorite-quartz with local kaolinite or pyrrhotite (Phillips and Law, 1994; Frimmel, 1997; Gartz and Frimmel, 1999). Such an assemblage is a typical metamorphic mineral assemblage, reflecting temperatures in excess of 300 °C (Phillips, 1986; Phillips and Law, 1994; Phillips and Powell, 2015).

The concentration of atmospheric O_2 plays a major role on the stability of both primary and secondary mineral assemblages (Heinrich, 2015). Mineralogical assemblages of Witwatersrand-type gold deposits, which formed during low atmospheric oxygen levels, consist of pyrite and uraninite in which their stability was facilitated by high fH_2S ($> 10^{-5}$) (Rasmussen and Buick, 1999). Within the reducing atmosphere regime, evidence of atmospheric oxygen whiffs has been recorded (Lyons et al., 2014; Frimmel and Hennigh, 2015). This is supported by molybdenum (Mo) isotope data, which proved the existence of Mn-oxides in 3.0 Ga seawater (Planavsky et al., 2014). A negative Ce-anomaly was also recorded in a 2.8 Ga biogenic limestone (Riding et al., 2014). In addition, Cr-isotopes and redox-sensitive metals in 3.0 Ga palaeosols and BIFs showed the probable, although not definitive prevalence of oxygen oscillation during the Archaean, which would have permitted the stabilisation of various minerals (Crowe et al., 2013). The use of Cr-isotopes to constrain atmospheric conditions is still debatable, as depending on the circumstance, heavy Cr isotopes may be associated with a marine setting and therefore not indicative of atmospheric oxygen levels (Albut et al., 2018). Therefore, Cr-isotopic results should ideally be co-constrained with other lines of evidence. Evidence from microbially-induced sedimentary structures at 3.2 and 2.9 Ga provided prime evidence to support the dependence of specific mineral parageneses on atmospheric O_2 (Noffke et al., 2008). In contrast, mineralisation in the Tarkwa gold deposits, which postdate oxygenation of the atmosphere, is associated with Fe oxides (i.e., magnetite and hematite) and tourmaline, whereas pyrite and uraninite are absent (Law and Phillips, 2006). The youngest example of Witwatersrand-type gold deposits formed in an oxidising atmospheric regime is the Palaeoproterozoic (1.88–1.80 Ga) Kumpu Group, located within the Central Lapland Greenstone Belt in Finland (Eilu et al., 2003). Similar to the mineralisation present in the Tarkwa and Roraima deposits, the minerals associated with gold are magnetite and hematite. Other examples are listed in Fig. 10 together with their relative age estimates.

4.7.3. Gold-concentrating mechanism

Although the processes that led to Au and U mineralisation in the Black Reef Formation are contested, there has been evidence supporting that these elements were sourced from the immediate hinterland (Fig. 9C). This could have occurred through remobilisation of primary detrital mineral phases and redeposition in the Black Reef by active hydrocarbon fluids (Fuchs et al., 2016), or by primary mechanical processes that were followed by hydrothermal activity (Nwaila et al., 2019). Similar to Witwatersrand gold deposits, the strata (e.g., quartz arenites and pelitic rocks) overlying (i.e., hangingwall) and underlying (i.e., footwall) the conglomerate unit of the Black Reef Formation are poorly mineralised. Previous studies that focused on detrital heavy mineral suites (e.g. apatite, cassiterite, chromite, corundum, diamond, garnet, gold [debated], monazite, pyrite [debated], uraninite [debated] and zircon; Feather and Koen (1975), Phillips and Law (2000), Frimmel and Minter (2002), and Law and Phillips (2006)) of the pre-Black Reef rocks, such as the Ventersdorp Contact Reef and various other Witwatersrand reefs, suggested that the variation in morphology and trace element composition of these minerals is due to mechanical sorting and not fluid activity (Robb and Meyer, 1991, 1995; Koglin et al., 2010b; Large et al., 2013; Burron et al., 2018).

Counter arguments for 'detrital minerals' were presented by Phillips and Law (2000), who argued that alteration and changes in physico-chemical conditions can form similar minerals, e.g. an association of gold with round pyrite may reflect sulphidation of detrital Fe-oxide grains and precipitation of gold transported as sulphur complexes, whereas a correlation of uranium with detrital titanium minerals may reflect precipitation of uranium by reaction with Ti to form brannerite. This would fit well with post-depositional interpretation of chemical precipitation of gold and associated ore minerals in the Black Reef Formation (Fuchs et al., 2016). Many publications on the mineralogy and chemistry of the Witwatersrand rocks, which made use of the recent advances in mineralogical and isotopic techniques, clearly showed unambiguous evidence for the existence of detrital mineral phases such as uraninite and pyrite (Hofmann et al., 2009; Frimmel et al., 2014; Agangi et al., 2015).

Our current data support the existence of these detrital phases and they correlate well with gold (Frimmel and Minter, 2002; Nwaila et al., 2019). These detrital phases indicate protracted periods of sedimentary reworking and mineral concentration under oxygen-deficient conditions. Concentrically laminated pyrite from the Witwatersrand Supergroup is known to contain heavy trace element inclusions such as Sb, Mn, Au, Ag, Tl, Cu, Mo and Mn. Analysis of the content of the pyrites as well as the ratios of these elements can be used to infer the setting of pyrite formation (Koglin et al., 2010b; Large et al., 2013; Agangi et al., 2015). A similar distribution of trace elements, in pyrite, was observed in the Black Reef Formation conglomerates (Fuchs et al., 2016). Therefore, detrital mineral suites of the Black Reef Formation and their association with gold provide strong evidence that gold mineralisation in the Black Reef Formation resulted, at least partially, from sedimentary source rocks. Even though post-depositional hydrothermal fluids interacted with the hydrocarbons within the Black Reef Formation during regional metamorphism (Fuchs et al., 2016) and contributed to additional gold and uranium mineralisation (Nwaila et al., 2019), this does not inhibit primary recycling of gold from the underlying palaeoplacers.

Comparison with similar styles of mineralisation in the Pardo deposit, Canada, reveals the importance of weathering and favourably reworked fluvial conglomerates that rest on an erosional unconformity and where a corresponding Au-enriched Archaean hinterland existed (Whymark and Frimmel, 2017). Coeval Witwatersrand-type gold mineralisation, post the Archaean, indicates that this style of mineralisation exists across different eras, even though the size of the deposits does not match that of the Witwatersrand Basin. As described in the introduction, previous studies have suggested a range of sources of gold for Witwatersrand-type gold deposits and occurrences. These include mobilisation of background Au concentrated in the hinterland by *syn*-depositional surface waters (Frimmel, 2014), orogenic-type auriferous quartz veins (Griffis et al., 2002), altered hinterland granites (Klemd and Hallbauer, 1987), and post-depositional metamorphic devolatilisation reactions (Phillips and Law, 2000). A refutation of the hydrothermally-altered granite ages was presented by Klemd et al. (1994), who argued that most of the alteration is a result of sediment dewatering affecting both the granitoids and gold-bearing horizons; thus the hydrothermally altered granitoids do not support their role as a possible source for the sulphides, gold and carbon nodules of the Witwatersrand reefs. We propose that the primary source of Black Reef Formation gold is the earlier Witwatersrand reefs and that the initial gold concentrating mechanism was a response to changes in drainage patterns and deep fluvial incisions closer to the Black Reef Formation/Witwatersrand Basin subcrop positions (Fig. 9C). Tectonic evolution, post-depositional metamorphism and metasomatism during the Black Reef Formation's prolonged geological history will have altered most of the primary textural details in gold, uraninite and some of the overgrowth along the rim-edges of detrital zircon. All these demonstrate that understanding the composition of the hinterland and the mechanisms of how this type of gold deposit/occurrence forms, will likely improve exploration targeting and discovery of new deposits in regions that are currently underexplored.

5. Conclusion

Uranium-Pb age dating of zircon grains contained within the Black Reef Formation indicates that the sediment was derived from erosion of both granite-greenstone protosource terranes, and Witwatersrand conglomerates and quartz arenites. Evidence of protosource and sediment reworking is prevalent in the Black Reef, not only in the Carletonville Goldfield, but also throughout Witwatersrand-type gold deposits. Petrological analysis of pyrites contained within the Black Reef Formation, in association with their previously reported Re-Os signatures, indicates the significance of granite-greenstone rocks in the formation of conglomerate-hosted gold deposits. In the case of the zircon age spectra, dilution of a fraction of detrital zircon grains occurred due to recycling of the underlying Witwatersrand rocks and post-depositional alteration. Recycling of Witwatersrand sediments corroborates with the primary mechanism of gold concentration in the Black Reef Formation, and thus serves to establish multiple lines of evidence that favours the mechanical concentration of gold from granite-greenstone terranes and gold-rich clastic sequences into the younger sedimentary succession. The paucity of gold distal to the Black Reef/ Witwatersrand subcrop, indicates that gold transport distance and subsequent deposition was strongly controlled by localised palaeodrainage patterns and source proximity. Lack of Ventersdorp Supergroup zircon grains in the Black Reef Formation is due to the rarity of zircon grains in continental flood basalts or insufficient amount of samples. The diversity of protosource rocks underlying Witwatersrand-type gold deposits globally demonstrates the importance of Archaean/Palaeoproterozoic granite-greenstone terranes, especially those with elevated background concentration of gold.

Declaration of Competing Interest

The authors declare that they have no known competing financial interests or personal relationships that could have appeared to influence the work reported in this paper.

Acknowledgements

We are deeply indebted to the two anonymous reviewers who provided constructive remarks, comments and critics that we tried to address best. We would also like to express our thanks to Franco Pirajno for editorial handling. We are grateful to George Henry, Axel Hofmann, and Julie Bourdeau for their inputs during conceptualisation stages and help with reviewing the first draft of the manuscript. We would also like to thank subject matter experts in this field who have been instrumental in shaping our ideas, especially Hartwig Frimmel and Neil Phillips. Hartwig Frimmel provided insightful discussions and comments on the role of protosource rocks in the formation of Witwatersrand-type mineralisation and their links to ore forming processes. Neil Phillips provided critical guidance on various Witwatersrand Basin genetic models, global distribution of similar deposits, reviewed the draft manuscript and pointed us to the relevant literature. We acknowledge Robert Bolhar for his technical help with U–Th–Pb analysis. This research was financially supported by the Department of Science and Technology–National Research Foundation (DST-NRF) Centre of Excellence for Integrated Mineral and Energy Resource Analysis (CIMERA) Research Grant.

Appendix A. Supplementary data

Supplementary data to this article can be found online at https://doi.org/10.1016/j.oregeorev.2020.103572.

References

Agangi, A., Hofmann, A., Rollion-Bard, C., Marin-Carbonne, J., Cavalazzi, B., Large, R., Meffre, S., 2015. Gold accumulation in the Archaean Witwatersrand Basin, South Africa—Evidence from concentrically laminated pyrite. Earth Sci. Rev. 140, 27–53.

Andersen, T., Kristoffersen, M., Elburg, M.A., 2017. Visualizing, interpreting and comparing detrital zircon age and Hf isotope data in basin analysis – a graphical approach. Basin Res. 30 (1), 132–147.

Albut, G., Babechuk, M.G., Kleinhanns, I.C., Benger, M., Beukes, N.J., Steinhilber, B., Smith, A.J.B., Kruger, S.J., Schoenberg, R., 2018. Modern rather than Mesoarchaean oxidative weathering responsible for the heavy stable Cr isotopic signatures of the 2.95 Ga old Ijzermijn iron formation (South Africa). Geochim. Cosmochim. Acta 228, 157–189.

Andersen, T., Saeed, A., Gabrielsen, R.H., Olaussen, S., 2011. Provenance characteristics of the Brumunddal sandstone in the Oslo Rift derived from U-Pb, Lu–Hf and trace element analyses of detrital zircons by laser ablation ICMPS. Norw. J. Geol. 91, 1–18.

Armstrong, R.A., Compston, W., Retief, E.A., Williams, I.S., Welke, H.J., 1991. Zircon ion microprobe studies bearing on the age and evolution of the Witwatersrand Triad. Precambr. Res. 53, 243–266.

Barnicoat, A.C., Henderson, I.H.C., Knipe, R.J., Yardley, B.W.D., Napier, R.W., Fox, N.P.C., Kenyon, A.K., Muntingh, D.J., Winkler, K.S., Lawrence, S.R., Cornford, C., 1997. Hydrothermal gold mineralization in the Witwatersrand Supergroup. Nature 386, 820–824.

Barton, E.S., Hallbauer, D.K., 1996. Trace–element and U-Pb isotope compositions of pyrite types in the Proterozoic Black Reef, Transvaal Sequence, South Africa: Implications on genesis and age. Chem. Geol. Rev. 133, 173–199.

Biao, S., Nutman, A.P., Dunyi, L., Jiashan, W., 1996. 3800 to 2500 Ma crustal evolution in the Anshan area of Liaoning Province, northeastern China. Precambr. Res. 78, 79–94.

Black, L.P., Kamo, S.L., Allen, C.M., Davis, D.W., Aleinikoff, J.N., Valley, J.W., Mundil, R., Campbell, I.H., Korsch, R.J., Williams, I.S., Foudoulis, C., 2004. Improved 206Pb/ 238U microprobe geochronology by the monitoring of a trace–element–related matrix effect; SHRIMP, ID–TIMS, ELA–ICP–MS and oxygen isotope documentation for a series of zircon standards. Chem. Geol. 205, 115–140.

Black, L.P., Kamo, S.L., Williams, I.S., Mundil, R., Davis, D.W., Korsch, R.J., Foudoulis, C., 2003. The application of SHRIMP to Phanerozoic geochronology; a critical appraisal of four zircon standards. Chem. Geol. 200 (1–2), 171–188.

Brandl, G., Cloete, M., Anhaeusser, C.R., 2006. Archaean greenstone belts. In: Johnson M. R., Anhaeusser C.R., Thomas R.J. (Eds), The Geology of South Africa. Geological Society of South Africa. Council for Geoscience, Johannesburg, pp. 9–56.

Bumby, A.J., Eriksson, P.G., Catuneanum, O., Nelson, D.R., Rigby, M.J., 2012. Meso-Archaean and Palaeo-Proterozoic sedimentary sequence stratigraphy of the Kaapvaal Craton. Mar. Petr. Geol. 33, 92–116.

Burron, I., da Costa, G., Sharpe, R., Fayek, M., Gauert, C., Hofmann, A., 2018. 3.2 Ga detrital uraninite in the Witwatersrand Basin, South Africa: Evidence of a reducing Archean atmosphere. Geol. Soc. Am. Bull. 46, 295–298.

Button, A., 1981. The Transvaal Supergroup. In: Hunter, D.R. (Ed.), Precambrian of the Southern Hemisphere. Elsevier, Amsterdam, Netherlands, pp. 527–536.

Button, A., 1986. The Transvaal sub–basin of the Transvaal Sequence. In: Anhaeusser, C. R., Maske, S. (Eds.) Mineral Deposits of Southern Africa 1, pp. 811–817.

Button, A., Tyler, N., 1981. The character and economic significance of Precambrian paleoweathering and erosion surfaces in southern Africa. 75th Anniversary. Econ. Geol. 676–699.

Canfield, D.E., 2005. The early history of atmospheric oxygen: Homage to Robert M. Garrels. Annual Rev. Earth Planetary Sci. 33, 1–36.

Clendenin, C.W., Henry, G., Charlesworth, E.G., 1991. Characteristics of and influences on the Black Reef depositional sequence in the eastern Transvaal. S. Afr. J. Geol. 94, 321–327.

Coetzee, H.P.A. 1996. The Stratigraphy and Sedimentology of the Black Reef Quartzite Formation, Transvaal Sequence, in the Area of Carletonville and West Rand Goldfields. MSc Thesis, Potchefstroom University for Christian Higher Education, South Africa.

Costa, G., Hofmann, A., Agangi, A., 2020. A revised classification scheme of pyrite in the Witwatersrand Basin and application to placer gold deposits. Earth Sci. Rev. 201, 103064. https://doi.org/10.1016/j.earscirev.2019.103064.

Crowe, S.A., Døssing, L.N., Beukes, N.J., Bau, M., Kruger, S.J., Frei, R., Canfield, D.E., 2013. Atmospheric oxygenation three billion years ago. Nature 501, 535–539.
Davidson, C.F., Cosgrove, M.E., 1955. On the impersistence of uraninite as a detrital mineral. Bull. Geol. Surv. Great Britain 10, 74–80.
de Wit, M.J., Armstrong, R.A., Kamo, S.L., Erlank, A.J., 1993. Gold bearing sediments in the Pietersberg greenstone belt: age equivalents of the Witwatersrand Supergroup sediments. Econ. Geol. 88, 1242–1252.
Dirks, P.H.G.M., Charlesworth, E.G., Munyai, M.R., Wormald, R., 2013. Stress analysis, post–orogenic extension and 3.01 Ga gold mineralisation in the Barberton Greenstone Belt, South Africa. Precambr. Res. 226, 157–184.
Dorfel, D., 1904. The Kromdraai Quartz Reef and its geological association. Trans. Geol. Soc. South Africa 6, 101–103.
Dunn, S.C., von der Heyden, B.P., Rozendaal, A., Taljaard, R., 2019. Secondary gold mineralisation in the Amani Gold Placer Deposit, Tanzania. Ore Geol. Rev. 107, 87–107.
Dvoretzky, A., Kiefer, J., Wolfowitz, J., 1956. Asymptotic minimax character of the sample distribution function and of the classical multinomial estimator. Ann. Math. Stat. 27, 642–669.
Dziggel, A., Kisters, A.F.M., 2019. Tectono-metamorphic controls on Archaean gold mineralization in the Barberton greenstone belt, South Africa. Developments in Precambrian Geology. Chapter 26 In: The Earth's Oldest Rocks. Elsevier, pp. 655–673.
Dziggel, A., Poujol, M., Otto, A., Kisters, A.F.M., Trieloff, M., Schwarz, W.H., Meyer, F.M., 2010. New U-Pb and $^{40}Ar/^{39}Ar$ ages from the northern margin of the Barberton greenstone belt, South Africa: implications for the formation of Mesoarchaean gold deposits. Precambr. Res. 179, 206–220.
Eglington, B.M., Armstrong, R.A., 2004. The Kaapvaal Craton and adjacent orogens, southern Africa: a geochronological database and overview of the geological development of the craton. S. Afr. J. Geol. 107 (1–2), 13–32.
Eilu, P., Sorjonen-Ward, P., Nurmi, P., Niiranen, T., 2003. A review of gold mineralization styles in Finland. Econ. Geol. 98 (7), 1329–1353.
Els, B.G., Van den Berg, W.A., Mayer, J.J., 1995. The Black Reef Formation in the Western Transvaal — sedimentological and economic aspects, and significance for basin evolution. Miner. Deposita 30, 112–123.
Endo, I., Machado, R., 2002. Reavaliac¸ ão e novos dados geocronológicos (Pb/Pb eK/Ar) da região do Quadrilátero Ferrífero e adjacências. Geol. USP Sér. Cient. 2, 23–40.
England, G.L., Rasmussen, B., Krapez, B., Groves, D.I., 2002. Palaeoenvironmental significance of rounded pyrite in siliciclastic sequences of the Late Archaean Witwatersrand Basin: oxygen–deficient atmosphere or hydrothermal alteration? Sedimentology 49, 1133–1156.
Eriksson, P.G., Altermann, W., Catuneanu, O., Van der Merwe, R., Bumby, A.J., 2001. Major influences on the evolution of the 2.67–2.1 Ga Transvaal Basin, Kaapvaal Craton. Sed. Geol. 141–142, 205–231.
Eriksson, P.G., Altermann, W., Hartzer, F.J., 2006. The Transvaal Supergroup and precursors. In: Johnson, M.R., Anhaeusser, C.R., Thomas, R.J. (Eds.), The Geology of South Africa. Geol. Society of South Africa, Johannesburg, pp. 237–260.
Eriksson, P.G., Reczko, B.F.F., 1995. The sedimentary and tectonic setting of the Transvaal Supergroup floor rocks to the Bushveld complex. J. Afr. Earth Sci. 21, 487–504.
Eriksson, P.G., Hattingh, P.J., Altermann, W., 1995. An overview of the geology of the Transvaal Sequence and Bushveld Complex, South Africa. Miner. Deposita 30, 98–111.
Farquhar, J., Bao, H., Thiemens, M., 2000. Atmospheric influence of Earth's earliest sulfur cycle. Science 289, 756–758.
Feather, C.E., Koen, G.M., 1975. The mineralogy of the Witwatersrand reefs. Mineral Sci. Eng. 7, 189–224.
Frankel, J.J., 1940. Notes on some of the minerals in the Black Reef series. Trans. Geol. Soc. South Africa 43, 1–11.
Frey, M., Germs, G.J.B., 1986. Some sedimentological observations on the conglomerates of the Black Reef Formation, Transvaal Supergroup, South Africa. Geocongress '86 Extended Abstracts, 993–995.
Frimmel, H.E., 2005. Archaean atmospheric evolution: evidence from the Witwatersrand gold fields, South Africa. Earth-Sci. Rev. 70, 1–46.
Frimmel, H.E., 2014. A giant Mesoarchaean crustal gold–enrichment episode: Possible causes and consequences for exploration. Soc. Econ. Geol. Spec. Publ. 18, 209–234.
Frimmel, H.E., 1997. Detrital origin of hydrothermal Witwatersrand gold – a review. Terra Nova 9, 192–197.
Frimmel, H.E., 2018. Episodic concentration of gold to ore grade through Earth's history. Earth-Sci. Rev. 180, 148–158.
Frimmel, H.E., Hennigh, Q., 2015. First whiffs of atmospheric oxygen triggered onset of crustal gold cycle. Miner. Deposita 50, 5–23.
Frimmel, H.E., Nwaila, G.T., 2020. Geologic evidence of syngenetic gold in the Witwatersrand Goldfields, South Africa. In Sillitoe, T., Goldfarb, R., Robert, F., Simmons, S. (eds.) Geology of the Major Gold Deposits and Provinces of the World. Society of Economic Geologists Special Publication xxx. In press.
Frimmel, H.E., Minter, W.E.L., 2002. Recent developments concerning the geological history and genesis of the Witwatersrand gold deposits, South Africa. Soc. Econ. Geol. Spec. Publ. 9, 17–45.
Frimmel, H.E., Groves, D.I., Kirk, J., Ruiz, J., Chesley, J., Minter, W.E.L., 2005. The formation and preservation of the Witwatersrand goldfields, the largest gold province in the world. In: Hedenquist, J.W., Thompson, J.F.H., Goldfarb, R.J., Richards, J.P. (Eds.), Economic Geology One Hundredth Anniversary Volume. Society of Economic Geologists, Littleton, pp. 769–797.
Frimmel, H.E., Schedel, S., Brätz, H., 2014. Uraninite chemistry as forensic tool for provenance analysis. Appl. Geochem. 48, 104–121.
Frimmel, H.E., Zeh, A., Lehrmann, B., Hallbauer, D.K., Frank, W., 2009. Geochemical and geochronological constraints on the nature of the immediate basement beneath the Mesoarchaean auriferous Witwatersrand Basin, South Africa. J. Petrol. 50, 2187–2220.
Fuchs, S., Williams-Jones, A.E., Jackson, S.E., Przybylowicz, W.J., 2017. Trace element chemistry of pyrobitumen from the Tau-Tona mine in South Africa. PANGAEA. Supplement to: Fuchs, S et al. (2016): Metal distribution in pyrobitumen of the Carbon Leader Reef, Witwatersrand Supergroup, South Africa: Evidence for liquid hydrocarbon ore fluids. Chem. Geol., 426. pp. 45–59.
Fuchs, S., Williams-Jones, A.E., Przybylowicz, W.J., 2016. The origin of the gold and uranium ores of the Black Reef Quartzite Formation, Transvaal Supergroup, South Africa. Ore Geol. Rev. 72, 149–164.
Garayp, E., Minter, W.E.L., Renger, F.E., Siegers, A., 1991. Moeda placer gold deposits in the Ouro Fino Syncline, Quadrilátero Ferrífero, Brazil. In: Ladeira, E.A. (Ed.), Proceedings of Brazil Gold '91; The Economics, Geology, Geochemistry and Genesis of Gold Deposits, pp. 601–608.
Gartz, V.H., Frimmel, H.E., 1999. Complex metasomatism of an Archean placer in the Witwatersrand Basin, South Africa: the Ventersdorp Contact Reef; a hydrothermal aquifer? Econ. Geol. 95 (5), 689–706.
Gauert, C.D.K., Deacon, J., Fuchs, S. 2010. Mineralogy and geochemistry of the Black Reef Au mineralisation at Cons. Modder, East Rand, South Africa. IMA 2010, Budapest. Acta Mineral. Petrograph. Abstract Series, Szeged 6, 302.
Germs, G.J.B. 1982. A paleogeographical study of the Black Reef Formation of the Transvaal Supergroup in the Venterdorp–Balfour area. JCI (Johannesburg Consolidated Investment) Report, (136).
Gold, D.J.C., 2006. The Pongola Supergroup, in: Johnson, M.R., Anhaeusser, C.R., Thomas, R.J. (Eds.), The Geology of South Africa. Geological Society of South Africa, pp. 135–147.
Griffis, R.J., Barning, K., Agezo, F.L., Akosah, F.K., 2002. Gold deposits of Ghana, Minerals Commission, Accra, 432 pp.
Gumsley, A.P., Chamberlain, K.R., Bleeker, W., Soderlund, U., de Kork, M.O., Larsson, E.R., Bekker, A., 2017. Timing and tempo of the Great Oxidation Event. Pro. Nat. Acad. Sci. 114, 1811–1816.
Gumsley, A.P., Stamsnijder, J., Larsson, E., Söderlund, U., Naeraa, T., de Kock, M.O., Ernst, R., 2018. The 2789–2782 Ma Klipriviersberg large igneous province: implications for the chronostratigraphy of the Ventersdorp Supergroup and the timing of Witwatersrand gold deposition. Geocongress 2018, 18–20 July 2018, Johannesburg, Geological Society of South Africa, Abstract Book, p. 133.
Hallbauer, D.K., Gehlen, K.V., 1983. The Witwatersrand pyrites and metamorphism. Mineralogical Magazine 47(345), 473–479.
Hart, R.J., Andreoli, M.A., Tredoux, M., De Wit, M.J., 1990. Geochemistry across an exposed section of Archean crust at Vredefort, South Africa: with implications for mid-crustal discontinuities. Chemical Geology 82, 21–50.
Heinrich, C.A., 2015. Witwatersrand gold deposits formed by volcanic rain, anoxic rivers and Archaean life. Nat. Geosci. 8, 206–209.
Henry, G., Clendenin, C.W., Charlesworth, E.G., 1990. Depositional facies of the Black Reef Formation in the eastern Transvaal. Geocongress '90 Abstract (Cape Town, South Africa), 230–233.
Hofmann, A., Anhaeusser, C.R., Dixon, J., Kröner, A., Saha, L., Wilson, A., Xie, H., 2019. Archaean granitoid–greenstone geology of the southeastern part of the Kaapvaal Craton. In: Kröner A., Hofmann A. (Eds) The Archaean Geology of the Kaapvaal Craton, Southern Africa. Regional Geology Reviews. Springer, Cham. pp. 33–54.
Hofmann, A., Bekker, A., Rouxel, O., Rumble, D., Master, S., 2009. Multiple sulphur and iron isotope composition of detrital pyrite in Archaean sedimentary rocks: A new tool for provenance analysis. Earth Planetary Sci. Lett. 286, 436–445.
Horscroft, F.D.M., Mossman, D.J., Reimer, T.O., Hennigh, Q., 2011. Witwatersrand metallogenesis: the case for (modified) syngenesis. SEPM Special Publication 101, 75–95.
Hunter, D.R., Johnson, M.R., Anhaeusser, C.R., Thomas, R.J., 2006. Introduction, in: Johnson, M.R., Anhaeusser, C.R., Thomas, R.J. (Eds.), Geology of South Africa. Geological Society of South Africa, pp. 1–8.
Jackson, M.C., 1992. A review of the late Archean volcano–sedimentary Dominion Group and implications for the tectonic setting of the Witwatersrand Supergroup, South Africa. J. Afr. Earth Sci. (Middle East) 15, 169–186.
Jackson, S.E., Pearson, N.J., Griffin, W.L., Belousova, E.A., 2004. The application of laser ablation–inductively coupled plasma–mass spectrometry to in situ U-Pb zircon geochronology. Chem. Geol. 211, 47–69.
Kamo, S.L., Key, R.M., Daniels, L.R.M., 1995. New evidence for Neoarchaean hydrothermally altered granites in south–central Botswana. J. Geol. Soc. London 152, 747–750.
Kerr, G., Malloch, K., Lilly, K., Craw, D., 2017. Diagenetic alteration of a Mesozoic fluvial gold placer deposit, southern New Zealand. Ore Geol. Rev. 83, 14–29.
Kinny, P.D., Maas, R., 2003. Lu–Hf and Sm–Nd isotope systems in zircon. In: Hanchar, J. M., Hoskin, P.W.O. (Eds.), Zircon. Reviews in Mineralogy and Geochemistry 53, Mineralogical Society of America, pp. 327–341.
Kirk, J., Ruiz, J., Chesley, J., Walshe, J., England, G., 2002. A major Archean gold and crust–forming event in the Kaapvaal Craton, South Africa. Science 297, 1856–1858.
Klemd, R., Hallbauer, D.K., 1987. Hydrothermally altered peraluminous Archaean granites as a provenance model for Witwatersrand sediments. Miner. Deposita 22, 227–235.
Klemd, R., Wülbers, A., Hallbauer, D.K., Barton Jr., J.M., 1994. Evidence for the origin of hydrothermal alteration in granitoids after Witwatersrand basin deposition, South Africa. Aust. J. Earth Sci. 41 (2), 131–140.
Koglin, N., Frimmel, H.E., Minter, W.E.L., Brätz, H., 2010a. Trace–element characteristics of different pyrite types in Mesoarchaean to Palaeoproterozoic placer deposits. Miner. Deposita 45, 259–280.
Koglin, N., Zeh, A., Cabral, A.R., Gomes Jr, A.A.S., Neto, A.V.C., Brunetto, W.J., Galbiatti,

H., 2014. Depositional age and sediment source of the auriferous Moeda Formation, Quadrilátero Ferrífero of Minas Gerais, Brazil: New constraints from U-Pb–Hf isotopes in zircon and xenotime. Precambr. Res. 255, 96–108.
Koglin, N., Zeh, A., Frimmel, H.E., Gerdes, A., 2010b. New constraints on the auriferous Witwatersrand sediment provenance from combined detrital zircon U-Pb and Lu–Hf isotope data for the Eldorado Reef (Central Rand Group, South Africa). Precambr. Res. 183, 817–824.
Kositcin, N., Krapež, B., 2004. SHRIMP U-Pb detrital zircon geochronology of the Late Archaean Witwatersrand Basin of South Africa: relation between zircon provenance age spectra and basin evolution. Precambr. Res. 129, 141–168.
Kristoffersen, M., 2017. U-Pb and Lu–Hf systematics of Detrital Zircon as a Sedimentary Provenance Indicator. PhD thesis. University of Oslo, Norway.
Krupp, R.K., Oberthür, T., Hirdes, W., 1994. The early Precambrian atmosphere and hydrosphere: Thermodynamic constraints from mineral deposits. Econ. Geol. Bull. Soc. Econ. Geol. 89, 1581–1598.
Large, R.R., Meffre, S., Burnett, R., Guy, B., Bull, S., Gilbert, S., Goemann, K., Danyushevsky, L., 2013. Evidence for an intrabasinal source and multiple concentration processes in the formation of the Carbon Leader reef, Witwatersrand Supergroup, South Africa. Econ. Geol. 108, 1215–1241.
Law, J.D., Phillips, N.G., 2006. Witwatersrand gold–pyrite–uraninite deposits do not support a reducing Archean atmosphere. Geol. Soc. Am. Memoirs 198, 121–141.
Liebenberg, W.R., 1955. The occurrence and origin of gold and radioactive minerals in the Witwatersrand System, the Dominion Reef, the Venetersdorp Contact Reef and the Black Reef. Trans. Geol. Soc. South Africa 58, 223–239.
Lyons, T., Reinhard, C., Planavsky, N., 2014. The rise of oxygen in Earth's early ocean and atmosphere. Nature 506, 307–315.
Maas, R., Kinny, P.D., Williams, I.S., Froude, D.O., Compston, W., 1992. The Earth's oldest known crust: a geochronological and geochemical study of 3900–4200 Ma old detrital zircons from Mt. Narryer and Jack Hills, Western Australia. Geochim. Cosmochim. Acta 56, 1281–1300.
Machado, N., Schrank, A., Noce, C.M., Gauthier, G., 1996. Ages of detrital zircon from Archean-Paleoproterozoic sequences: implications for Greenstone Belt setting evolution of a Transamazonian foreland basin in Quadrilátero Ferrífero, southeast Brazil. Earth Planet. Sci. Lett. 141, 259–276.
Marsh, J.S. 2006. The Dominion Group. In: Johnson, M.R., Anhaeusser, C.R., Thomas, R. J. (Eds.), Geology of South Africa. Geological Society of South Africa, pp. 149–154.
Martin, D.M., Clendenin, C.W., Krapez, B., McNaughton, N.J., 1998. Tectonic and geochronological constraints on late Archaean and Palaeoproterozoic stratigraphic correlation within and between the Kaapvaal and Pilbara Cratons. J. Geol. Soc. London 155, 311–322.
Maynard, J.B., Ritger, S.D., Sutton, S.J., 1991. Chemistry of sands from the modern Indus River and the Archean Witwatersrand basin: Implications for the composition of the Archean atmosphere. Geology 19, 265–268.
McCarthy, T.S. 2006. The Witwatersrand Supergroup. In: Johnson, M.R., Anhaeusser, C. R., Thomas, R.J. (Eds.), Geology of South Africa. Geological Society of South Africa, pp. 155–186.
McLoughlin, A., Blignaut, L., Viljoen, F. 2014. A geometallurgical examination of gold, uranium and thorium in the Black Reef quartzite formation. Abstracts 21st General Meeting of the International Mineralogical Association (IMA2014), Johannesburg, South Africa, 1–5 September 2014, ISBN: 978-0-620-60082-8, p. 122.
Milesi, J.P., Ledru, P., Marcoux, E., Johan, V., Lerouge, C., Sabate, P., Bailly, L., Respaut, J.P., Skipwith, P., 2002. The Jacobina Paleoproterozoic gold–bearing conglomerates, Bahia, Brazil: A 'hydrothermal shear–reservoir' model. Ore Geol. Rev. 19, 95–136.
Minter, W.E.L. 1978. A sedimentological synthesis of placer gold, uranium and pyrite concentrations in Proterozoic Witwatersrand sediments. In: Miall, A.D. (ed.), Fluvial Sedimentology Memoir, Canadian Society Petroleum Geology 5, 801–829.
Mossman, D.J., Harron, G.A, 1983. Origin and distribution of gold in the Huronian Supergroup, Canada — the case for Witwatersrand-type paleoplacers. Precambrian Res. 20, 543–583. https://doi.org/10.1016/0301-9268(83)90089-X.
Mossman, D.J., Minter, W.E.L., Dutkiewicz, A., Hallbauer, D.K., George, S.C., Hennigh, Q., Reimer, T.O., Horscroft, F.D., 2008. The indigenous origin of Witwatersrand "carbon". Precambr. Res. 164, 173–186.
Noffke, N., Beukes, N., Bower, D., Hazen, R.M., Swift, D.J.P., 2008. An actualistic perspective into Archean worlds—(cyano–)bacterially induced sedimentary structures in the siliciclastic Nhlazatse section, 2.9 Ga Pongola Supergroup, South Africa. Geobiology 6, 5–20.
Nwaila, G.T., Bourdeau, J.E., Jinnah, Z., Frimmel, H.E., Bybee, G.M., Zhang S.E., Manzi, M.S.D., Minter, W.E.L., Mashaba, D., 2020. The Significance of Erosion Channels on Gold Metallogeny in the Witwatersrand (South Africa): Evidence from the Carbon Leader Reef in the Carletonville Goldfield. Economic Geology xxx, in press.
Nwaila, G.T., Frimmel, H.E., 2019. Highly siderophile elements in Archaean and Palaeoproterozoic marine shales of the Kaapvaal Craton, South Africa. Mineral. Petrol. 113, 307–327.
Nwaila, G.T., Frimmel, H.E., Minter, W.E.L., 2017. Provenance and geochemical variations in shales of the Mesoarchaean Witwatersrand Supergroup. J. Geol. 125, 399–422.
Nwaila, G.T., Manzi, M.S.D., Kirk, J., Maselela, H.K., Durrheim, R.J., Rose, D.H., Nwaila, P.C., Bam, L.C., Khumalo, T., 2019. Recycling of paleoplacer gold through mechanical and postdepositional mobilization in the Neoarchean Black Reef Quartzite Formation, South Africa. J. Geol. 127, 137–166.
Oberthür, T., Hirdes, W., Höhndorf, A., Schmidt Mumm, A., Vetter, U., Weiser, T., Davis, D.W., Blenkinsop, T.G., Amanor, J.A., Loh, G., 1995. A review of gold mineralisation in the Ashanti Belt of Ghana and its relation to the crustal evolution of the terrane. Commun. Geol. Survey Namibia 10, 121–127.
Oberthür, T., Vetter, U., Davis, D.W., Amanor, J.A., 1998. Age constraints on gold mineralization and Paleoproterozoic crustal evolution in the Ashanti belt of southern Ghana. Precambr. Res. 89, 129–143.
Ohmoto, H., 1996. Evidence in pre–2.2 Ga paleosols for the early evolution of atmospheric oxygen and terrestrial biota. Geology 24, 1135–1138.
Palmer, J.A., Phillips, G.N., McCarthy, T.S., 1987. The nature of the Precambrian atmosphere and its relevance to Archaean gold mineralization. In Ho, S.E., and Groves, D. I., (Eds), Recent Advances in Understanding Precambrian Gold Deposits. Perth, Geology Department and Extension, University of Western Australia, Publication 11, 327–340.
Palmer, J.A., Phillips, G.N., McCarthy, T.S., 1989. Paleosols and their relevance to Precambrian atmospheric composition. J. Geol. 97, 77–92.
Papenfus, J.A. 1964. The Black Reef Series within the Witwatersrand basin with special reference to its occurrence at Government Gold mining areas. In: Haughton, S.H. (Ed.), The Geology of some Ore Deposits in South Africa. Geological Society of South Africa 191–218.
Paton, C., Hellstrom, J., Paul, B., Woodhead, J., Hergt, J., 2011. Iolite: freeware for the visualisation and processing of mass spectrometric data. J. Anal. At. Spectrom. 26, 2508.
Paton, C., Woodhead, J.D., Hellstrom, J.C., Hergt, J.M., Greig, A., Maas, R., 2010. Improved laser ablation U-Pb zircon geochronology through robust downhole fractionation correction. Geochem. Geophys. Geosyst. 11 (3).
Perrouty, S., Aillères, L., Jessell, M.W., Baratoux, L., Bourassa, Y., Crawford, B., 2012. Revised Eburnean geodynamic evolution of the gold–rich southern Ashanti Belt, Ghana, with new field and geophysical evidence of pre–Tarkwaian deformations. Precambr. Res. 204–205, 12–39.
Petrus, J.A., Kamber, B.S., 2012. VizualAge: A novel approach to laser ablation ICP-MS U-Pb geochronology data reduction. Geostand. Geoanal. Res. 36, 247–270.
Phillips, G.N., 1986. Metamorphism of shales in the Witwatersrand goldfields. Economic Geology Research Unit, University of the Witwatersrand. Information Circular No. 192, pp. 29.
Phillips, G.N., 1987. Metamorphism of the Witwatersrand gold fields: conditions during peak metamorphism. J. Metamorph. Geol. 5, 307–322.
Phillips, G.N., Law, J.D.M., 1994. Metamorphism of the Witwatersrand Gold Fields — a review. Ore Geol. Rev. 9, 1–31.
Phillips, G.N., Law, J.D.M., 2000. Witwatersrand goldfields: Geology, genesis and exploration. In: Hagemann, S.G. and Brown, P.E., (Eds), Gold in 2000. Society of Economic Geology Reviews, 13, 439–500.
Phillips, G.N., Myers, R.E., 1989. The Witwatersrand goldfields, II: An origin for Witwatersrand gold during metamorphism and associated alteration. Econ. Geol. Monogr. 6, 598–608.
Phillips, G.N., Powell, R., 2015. Hydrothermal alteration in the Witwatersrand goldfields. Ore Geol. Rev. 65, 245–273.
Pitcairn, I.K., 2011. Background concentrations of gold in different rock types. Appl. Earth Sci. 120, 31–38.
Planavsky, N.J., Asael, D., Hofmann, A., Reinhard, C.T., Lalonde, S.V., Knudsen, A., Wang, X., Ossa Ossa, F.O., Pecoits, E., Smith, A.J.B., Beukes, N.J., Andrey Bekker, A., Johnson, T.M., Konhauser, K.O., Lyons, T.W., Rouxel, O.J., 2014. Evidence for oxygenic photosynthesis half a billion years before the Great Oxidation Event. Nat. Geosci. 7, 283–286.
Poujol, M., Anhaeusser, C.R., 2001. The Johannesburg Dome, South Africa, new single zircon U-Pb isotopic evidence for early Archaean granite–greenstone development within the central Kaapvaal Craton. Precambr. Res. 108, 139–157.
Poujol, M., Robb, L.J., Anhaeusser, C.R., Gericke, B., 2003. A review of the geochronological constraints on the evolution of the Kaapvaal Craton, South Africa. Precambr. Res. 127, 181–213.
Pretorius, D.A., 1981. Gold and uranium in quartz–pebble conglomerates. 75th Anniversary Volume. Econ. Geol. 117–138.
Pretorius, D.A., 1991. The sources of Witwatersrand gold and uranium: A continued difference of opinion. In: Hutchinson, R.W., and Grauch, R.I., (Eds), Historical pPerspectives of Genetic Concepts and Case Histories of Famous Discoveries. Economic Geology Monograph 8, 139–163.
Rasmussen, B., Buick, R., 1999. Redox state of the Archean atmosphere: Evidence from detrital heavy minerals in ca. 3250–2750 Ma sandstones from the Pilbara Craton, Australia. Geology 27, 115–118.
Renik, B., Christie-Blick, N., Troxel, B.W., Wright, L.A., Niemi, N.A., 2008. Re–evaluation of the middle Miocene Eagle Mountain Formation and its significance as a piercing point for the interpretation of extreme extension across the Death Valley region, California, U.S.A. J. Sediment. Res. 78, 199–219.
Riding, R., Fralick, P., Liang, L., 2014. Identification of an Archean marine oxygen oasis. Precambr. Res. 251, 232–237.
Robb, L.J., Davis, D.W., Kamo, S.L., 1990. U-Pb ages on single detrital zircon grains from the Witwatersrand Basin, South Africa: constraints on the age of sedimentation and the evolution of granites adjacent to the basin. J. Geol. 98, 311–328.
Robb, L.J., Davis, D.W., Kamo, S.L., Meyer, F.M., 1992. Ages of altered granites adjoining the Witwatersrand Basin with implications for the origin of gold and uranium. Nat. Geosci. 357, 677–680.
Robb, L.J., Meyer, F.M., 1991. A contribution to recent debate concerning epigenetic versus syngenetic mineralization processes in the Witwatersrand Basin. Econ. Geol. 86, 396–401.
Robb, L.J., Meyer, F.M., 1995. The Witwatersrand Basin, South Africa: geological framework and mineralisation processes. Ore Geol. Rev. 10, 67–94.
Schiøtte, L., Compston, W., Bridgwater, D., 1988. Late Archean ages for the deposition of clastic sediments belonging to the Malene supracrustals, southern West Greenland: evidence from an ion probe U-Pb zircon study. Earth Planet. Sci. Lett. 87, 45–58.
Schmitz, M.D., Bowring, S.A., De Wit, M.J., Gartz, V., 2004. Subduction and terrane collision stabilized the Kaapvaal Craton tectosphere 2.9 billion years ago. Earth Planet. Sci. Lett. 222, 363–376.

Sircombe, K.N., Stern, R.A., 2002. An investigation of artificial biasing in detrital zircon U-Pb geochronology due to magnetic separation in sample preparation. Geochim. Cosmochim. Acta 66, 2379–2397.
Sláma, J., Košler, J., Condon, D.J., Crowley, J.L., Gerdes, A., Hanchar, J.M., Horstwood, M.S., Morris, G.A., Nasdala, L., Norberg, N., Schaltegger, U., 2008. Plešovice zircon—a new natural reference material for U-Pb and Hf isotopic microanalysis. Chem. Geol. 249, 1–35.
Smith, A.J.B., Henry, G., Frost-Killian, S., 2016. A review of the Birimian Supergroup– and Tarkwaian Group–hosted gold deposits of Ghana. Episodes 39 (2), 177–179.
mith, W. 2006. Gold Mine. St. Martin's Paperbacks (first published 1970). p. 272.
Stonestreet, C.D., 1898. Notes on the Black Reef at Natal Spruit. Trans. Geol. Soc. South Africa 2, 53–55.
Sumner, D.Y., Beukes, N.J., 2006. Sequence stratigraphic development of the Neoarchean Transvaal carbonate platform, Kaapvaal Craton, South Africa. S. Afr. J. Geol. 109, 11–22.
Sutton, S.J., Ritger, S.D., Maynard, J.B., 1990. Stratigraphic control of chemistry and mineralogy in metamorphosed Witwatersrand quartzites. J. Geol. 98, 329–341.
Swiegers, J.U., 1938. A study ofthe Black Reef Series in the KIerksdorp and Randfontein areas. Trans. Geol. Soc. South Africa 41, 177–191.
Swiegers, J.U., 1939. Gold, carbon, pyrite and other sulphides in the Black Reef. Trans. Geol. Soc. South Africa 42, 35–46.
Tankard, A.J., Jackson, M.P.A., Eriksson, K.A., Hobday, D.K., Hunter, D.R., Minter, W.E.L., 1982. Crustal Evolution of Southern Africa – 3.8 Billion Years of Earth History. Springer-Verlag, New York, pp. 523.
Van den Berg, W.A., 1994. Stratigraphy and Sedimentology of the Black Reef Quartzite Formation, Transvaal Sequence, in the KIerksdorp, Potchefstroom and Ventersdorp Districts. Unpublished M. Sc. Thesis, Potchefstroom University for Christian Higher Education, 131.
Vermeesch, P., 2012. On the visualisation of detrital age distributions. Chem. Geol. 312–313, 190–194.
Vermeesch, P., 2018. IsoplotR: a free and open toolbox for geochronology. Geosci. Front. 9, 1479–1493.
Viljoen, R., 1963. Petrographic and Mineragraphic Aspects of the Main Reef and Main Reef Leader. MSc thesis, University of the Witwatersrand, South Africa.
Visser, W.J. 1989. Sedimentologiese Ondersoek van die Swartrif Kwartseit Formasie in die Verre– Wes Rand. Gold Fields of South Africa, Unpublished Company Report, 29.
Walraven, F., Martini, J., 1995. Zircon Pb–evaporation age determinations of the Oak Tree Formation, Chuniespoort Group, Transvaal Sequence: implications for Transvaal Griqualand West basin correlations. South Afr. J. Geol. 98, 58–67.
Van der Westhuizen, W.A., de Bruiyn, H., Meintjes, P.G., 2006. The Ventersdorp Supergroup. In: Johnson, M.R., Anhaeusser, C.R., Thomas, R.J. (Eds.): The Geology of South Africa. Geological Society of South Africa Johannesburg and the Council for Geoscience Pretoria. pp. 187–208.
Wasserman, L., 2006. All of Nonparametric Statistics. Springer.
Wernicke, B., 2011. The California River and its role in carving Grand Canyon. Geol. Soc. Am. Bull. 123, 1288–1316.
Whymark, W., Frimmel, H.E., 2017. Regional gold–enrichment of conglomerates in Palaeoproterozoic supergroups formed during the 2.45 Ga rifting of Kenorland. Ore Geol. Rev. 101, 985–996.
Yao, Y., Robb, L.J., 2000. Gold mineralization in Paleoproterozoic granitoids at Obuasi, Ashanti region, Ghana: Ore geology, geochemistry and fluid characteristics. S. Afr. J. Geol. 103, 255–278.
Zeh, A., Ovtcharova, M., Wilson, A., Schaltegger, U., 2015. The Bushveld Complex was emplaced and cooled in less than one million years – results of zirconology, and geotectonic implications. Earth Planet. Sci. Lett. 418, 103–114.
Zhao, B., Robb, L., Harris, C., Jordaan, W., 2006. Origin of hydrothermal fluids and gold mineralization associated with the Ventersdorp Contact Reef, Witwatersrand Basin, South Africa: Constraints from S, O, and H isotopes. Special Paper Geol. Soc. Am. 405, 333–352.